

Modeling the two-way coupling between *Lanice conchilega* and sand waves on the bottom of the North Sea

Maris¹, H.L., Borsje², B.W., Damveld², J.H., Hulscher², S.J.M.H.

1 Student Water Engineering and Management

2 Graduation committee

Enschede, January 2018

**Modeling the two-way coupling between
Lanice conchilega and sand waves on the
bottom of the North Sea**



H.L. MARIS BSC
January 2018

UNIVERSITY OF TWENTE.

Modeling the two-way coupling between *Lanice conchilega* and sand waves on the bottom of the North Sea

Master Thesis
Marine and Fluvial systems
Water Engineering and Management
Faculty of Engineering Technology
University of Twente

Student: H.L. Maris Bsc

Location and date: Enschede, January 2018

Graduation supervisor: Prof. dr. S.J.M.H. Hulscher

Daily supervisors: Dr. Ir. B.W. Borsje
J.H. Damveld Msc

Image cover: *Lanice conchilega* worm

Copyright: Alex Hyde, Minden Pictures

Abstract

The tube-building worm *Lanice conchilega* is an ecosystem engineer, which affects its environment by changing the local hydrodynamics and therewith the sediment dynamics. The worm occurs in subtidal and intertidal areas and it lives in patches of hundreds per m^2 . They form mounds of 10-80 cm height in soft-bottom sediments. The goal of this study is to determine the effects of a two-way coupling between dynamic patches of *Lanice conchilega* and dynamically active sand waves on the bottom of the North Sea. The effects of *Lanice conchilega* onto sand waves are studied as well as the effects of the sand waves on the tubes. The numerical process-based model Delft3D has been used to study the two-way coupling.

The tubes are modeled as thin solid piles that affect drag and turbulence, thereby they affect the local sediment dynamics. The effects of *Lanice conchilega* on the local hydrodynamics and morphodynamics are investigated by modeling static patches with tubes on a flat bottom. The patches are also modeled in sand waves, to study the two-way coupling. The bathymetries consisted of a sinusoidal and a self-organizational bottom. The patches were located where the bed shear stress was lower than the mean tide-averaged bed shear stress for the model domain. The density of the patch was updated every season by a growth curve and the available suspended sediment. Furthermore, the patches disappeared every year, every five years, and never.

The protruding tubes from the sediment cause more bottom roughness, therefore, within the patch, the near-bottom flow is decreased and the turbulence is increasing to its maximum value which occurs at the top of the tubes. Due to the decrease of near bottom flow, sediment was deposited between the tubes and this forms mounds. At the leading edge (zero cm in front of the patch) erosion holes were formed due to an increased flow velocity. Because of tidal symmetry, the leading edge switches and erosion holes are formed at both sides of the patch.

Patches of *Lanice conchilega* were also implemented in sand waves. After one year of morphological development, both for the sinusoidal and self-organizational bottom, the bed level was only locally changed at the locations of the patches. The degradation rates of the mounds were different in troughs, half-way the flanks, and at local crests (only in self-organizational bottom), because of differences in bed shear stresses. After 20 years of morphological development the case where the patches disappeared every year was the most realistic case, because the mound heights were in agreement with field studies. Furthermore, for the self-organizational bottom, a smaller sand wave growth was shown for the bottom with patches compared to the bottom without patches.

Acknowledgements

This research is the final project of my studies Water Engineering & Management at the University of Twente. This model study describes the influence of patches of *Lanice conchilega* on sand waves in the North Sea. Looking back at the process it took me, to finalize this document, I enjoyed the modeling and all conversations I had about this topic.

First of all, I would like to thank my supervisors. Suzanne Hulscher for her suggestions on my results. Bas Borsje for giving me the opportunity to start on this topic and his guidance about how I should conduct this research. And last, I would like to thank Johan Damveld for the time he took for our many discussions and his help with the analysis of the results.

Furthermore, I would like to thank my friends and fellow students for all our lunch walks, coffee breaks and our conversations.

And finally, I would like to thank my parents, who gave me the opportunity to study and who always support me.

Henrike Maris
January, 2018

Contents

Abstract	iii
Acknowledgements	v
1 Introduction	1
1.1 Problem definition	2
1.2 Research objective	4
1.3 Method	4
1.4 Outline	4
2 Characteristics of <i>Lanice conchilega</i>	7
2.1 Introduction	7
2.2 Life cycle	7
2.3 Habitat	9
2.4 Field studies	9
2.5 Effects of tubes on hydrodynamics and sediment dynamics	10
3 Model set-up	13
3.1 Delft3D	13
3.1.1 Hydrodynamic equations	13
3.1.2 Sediment transport and bed evolution equations	14
3.2 Vegetation model	16
3.3 Grid	18
3.3.1 Flat bottom	18
3.3.2 Sinusoidal bottom	18
4 Inclusion of biological activity	21
4.1 Growth factors	21
4.1.1 Tube density growth	21
Recruitment factor	21
Sediment factor	23
4.1.2 Bottom covering growth	23
4.2 Assumptions	24
4.3 Implementation of <i>Lanice conchilega</i> patches	25
5 Static patches on flat bottoms	29
5.1 Bathymetry	29
5.2 Method	29
5.3 Results	30
5.3.1 Reference case	30

	Hydrodynamics: Case I and II	30
	Morphodynamics: Case III and IV	33
5.3.2	Variable cases	35
	Case II: Variable tube density	35
	Case II: Variable tube length	36
	Case II: Variable patch length	37
	Case II: Multiple patches	37
	Case IV: Mound height for varying tube densities and lengths	39
5.4	Conclusion	42
6	Dynamic patches in sand waves	43
6.1	Bathymetry	43
6.2	Method	44
6.3	Results: Comparison sediment factors	45
6.4	Results: Morphological development	48
6.4.1	Sinusoidal bottom	48
	Option one after ten years	51
	Option two after ten years	52
	Option three after ten years	53
6.4.2	Self-organisational bottom	54
	Option two after twenty years	56
	Option three after twenty years	57
	Frequency domain	58
6.5	Conclusion	59
7	Discussion	61
8	Conclusion and recommendations	63
8.1	Conclusion	63
8.2	Recommendations	64
	Bibliography	67

List of Symbols

Delft3D symbols

A_p	[-]	solidity of the vegetation measured on a horizontal cross section at vertical level z
c	$[kgm^{-3}]$	mass concentration of sediment
c_μ	[-]	constant with a recommended value of 0.09 (Rodi, 1984)
$c_{2\epsilon}$	[-]	coefficient
c_μ	[-]	coefficient
C_l	[-]	coefficient reducing the geometrical length scale
D_{cyl}	$[m]$	diameter of the cylindrical structure
D_*	[-]	non-dimensional particle diameter
d	$[m]$	sediment grain size
F_r	$[Nm^{-3}]$	resistance force
F_u	$[ms^{-2}]$	horizontal Reynold's stresses
H	$[m]$	water depth
k	$[m^2s^{-2}]$	turbulent kinetic energy
M	[-]	sediment mobility number
M_e	[-]	excess sediment mobility number
n	$[m^{-2}]$	number of cylinders per unit area
P_u	$[Nm^{-2}]$	pressure gradient
S_b	$[kgm^{-1}s^{-1}]$	bed load transport (eq. 3.9)
S_s	$[kgm^{-1}s^{-1}]$	suspended load transport (eq. 3.14)
T	$[m^2s^{-2}]$	work spent by the fluid
u	$[ms^{-1}]$	horizontal velocity in x direction
u_c	[-]	efficiency factor, ratio between the grain related friction factor and the total current related friction factor
u_{cr}	$[ms^{-1}]$	critical depth-averaged velocity for the initiation of motion of sediment based on the shields curve
u_r	$[ms^{-1}]$	magnitude of the equivalent depth-averaged velocity computed from the velocity in the bottom computational layer assuming a logarithmic velocity profile
u_*	$[ms^{-1}]$	shear velocity that relates the velocity gradient at the bed to the velocity u in the lowest computational grid point by assuming a logarithmic velocity profile
z_b	$[m]$	upwards positively defined bed level

α_s	[-]	correction parameter of the slope effects
ϵ	$[m^2 s^{-3}]$	turbulent energy dissipation
ϵ_p	[-]	bed porosity with value 0.4
$\epsilon_{s,x}, \epsilon_{s,z}$	$[m^2 s^{-1}]$	sediment diffusivity coefficients in x and z direction
ζ	[m]	free surface elevation
λ_s	[-]	slope parameter, which is usually taken inversely proportional to the tangent of the angle of repose of sand (Sekine and Parker, 1992) leading to $\lambda_s = 2.5$
ν	$[m^2 s^{-1}]$	kinematic viscosity
ν_T	$[m^2 s^{-1}]$	eddy viscosity
ρ_s	$[kg m^{-3}]$	specific density of the sediment
ρ_w	$[kg m^{-3}]$	water density
τ_b	$[Nm^{-2}]$	bed shear stress
τ_{cr}	$[Nm^{-2}]$	critical bed shear stress for the initiation of motion of sediment
ω	$[s^{-1}]$	vertical velocity relative to the moving vertical $\sigma - plane$
ω_s	$[m s^{-1}]$	settling velocity of the sediment

Model symbols

$\langle c \rangle$	$[kg m^{-3}]$	tide-averaged suspended sediment concentration
C_{max}	[%]	maximum covering of the bottom
$C(t)$	[%]	covering at a specific moment in time
C_0	[%]	initial covering of the bottom
D	[ind. m^{-2}]	tube density
D_{max}	[ind. m^{-2}]	maximum density of <i>Lanice conchilega</i>
D_{tube}	[ind. m^{-2}]	tube density
$D_{tube,initial}$	[ind. m^{-2}]	initial tube density
$D(t)$	[ind. m^{-2}]	tube density at a specific moment in time
D_0	[ind. m^{-2}]	initial density of <i>Lanice conchilega</i>
d	$[\mu m]$	grain size
d_{tube}	[cm]	tube diameter
H	[m]	water depth
H_{wave}	[m]	wave height
L_{patch}	[m]	patch length
L_{tube}	[cm]	tube length
L_{wave}	[m]	wave length
R	[-]	recruitment factor
S	[-]	sediment factor
$S(\langle c \rangle)$	[-]	sediment factor dependent on the sediment concentration at a specific location
t	[days]	time
U_{S2}	$[ms^{-1}]$	tidal flow amplitude
$max\langle c \rangle$	$[kg m^{-3}]$	maximum tide-averaged suspended sediment concentration,
$mean\langle c \rangle$	$[kg m^{-3}]$	mean tide-averaged suspended sediment concentration in whole domain
α_g	$[m^2 ind.^{-1} days^{-1}]$	growth factor

β_g	$[\%^{-1} \text{ days}^{-1}]$	growth factor
$\langle \tau \rangle$	$[N \text{ m}^{-2}]$	tide-averaged bed shear stress
$\max \langle \tau \rangle$	$[N \text{ m}^{-2}]$	mean tide-averaged bed shear stress

CHAPTER 1

Introduction

Shallow coastal seas, such as the North Sea, are of high importance from both an economical and ecological point of view. They serve for a wide range of human activities and they form the habitat for a broad variety of organisms. Examples of human activities are; navigation of ships, offshore constructions, and pipes running through the sea. A good execution of these activities depend on an adequate understanding of the sediment dynamics. Shipping lines should have sufficient depth, constructions should have a proper foundation, and pipes should not become exposed due to migrating sand waves.

A wide range of regular bed patterns is shown in shallow coastal seas, among which sand waves and sand banks are the largest. Tidal sand waves have wave lengths of hundreds of meters and heights of tens of meters and they migrate with several meters a year. Tidal sand banks, however, hardly move. They have heights up to 30 meters and their length is between 5-10 kilometers (Hulscher, 1996).

Recently there has been an increasing interest in the feedback between organisms and sediment dynamics, which is also referred to as biogeomorphology (Murray et al., 2008; Corenblit et al., 2011). It has become clear that organisms can have a large influence on the sediment dynamics, by acting either as stabilizers or destabilizers (e.g. Widdows and Brinsley, 2002).

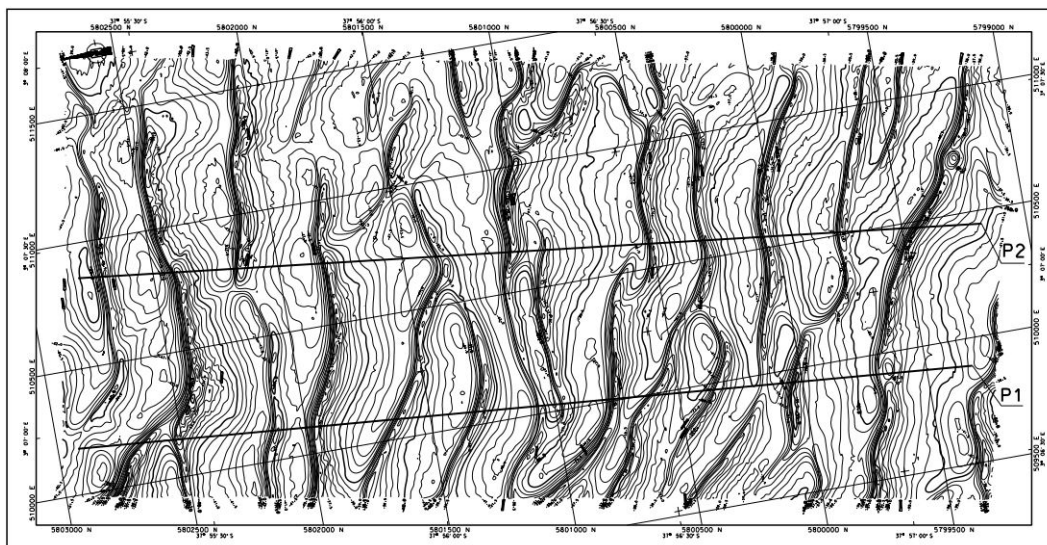


FIGURE 1.1: Bottom topography of a sand wave field in the North Sea (Besio et al., 2006).

It is important to study these effects, because they can improve the predictions of sand wave patterns. Model studies have improved the accuracy of determining the occurrence of sand waves as well as determining the wave length (Borsje et al., 2014b). However, model predictions of sand waves still need to be improved, for example inclusion of biological activity can be used.

This research is part of the SANDBOX program, which aims for unraveling the mechanisms behind the coupled seawater-seabed system. Within this program the impacts of offshore activities will be investigated on this system (Damveld et al., 2015).

1.1 Problem definition

Tidal sand waves are rhythmic and dynamic bed features, found in sandy shallow seas. The interaction between the sandy sea bottom and oscillatory currents gives rise to the initial formation of sand waves. Tidal sand waves are an important marine bed pattern, due to the combination of their dimensions, dynamics, and occurrence.

The initial behavior, like the initial growth rate, wave length, orientation, and migration speed (Besio et al., 2008), can be explained with linear terms in analytical models. Huthnance (1982) introduced a 2D model which could explain the formation of sand banks. Later on, Hulscher (1996) used another model in 3D, which could also explain the formation of sand waves. This model has been improved by Gerkema (2000) and Komarova and Hulscher (2000). Since then, various physical processes have been modeled; for example Németh et al. (2002) investigated surface wind stresses. Besio et al. (2003), Besio et al. (2004), Blondeaux and Vittori (2005a), and Blondeaux and Vittori (2005b) researched physical processes like currents, migration, and suspended sediment transport. Also grain sorting has been studied by van Oyen and Blondeaux (2008) and Roos et al. (2007).

However, non-linear effects become important when the amplitude increases. A non-linear model was proposed by Németh et al. (2007) and Sterlini et al. (2009), the sand waves were modeled towards their equilibrium shape in a two dimensional vertical model (2DV). Later on, Borsje et al. (2013) and Borsje et al. (2014b) modeled sand wave formation in a numerical shallow water model. In this model (Delft3D, (Lesser et al., 2004)) the same processes can be included as in the linear sand wave model. However, in this model non-linear effects can be included as well. This means that for example the equilibrium height of sand waves can be studied (Van Gerwen et al., 2016).

Recently, a lot of research has been done in biogeomorphology. Biogeomorphology is the interaction between two disciplines, biology and geomorphology. It became clear that animals have large effects on the sediment dynamics in shallow coastal seas (Meadows et al., 2012). They can strongly influence the local sediment composition, by acting as a stabilizer or destabilizer (Widdows and Brinsley, 2002). The inclusion of these living organisms into the modeling has made significant improvements in geomorphology (Corenblit et al., 2011). Originally this biogeomorphological research was only done in a one-way fashion. This manner only studied the effects of organisms on sediment transport and morphological change. However, it has become clear that sediment transport and morphological change can also affect biological development. Murray et al. (2008) state that this can just be as important as the other way around. Instead of a 'one-way' interaction, a 'two-way' interaction between biology and geomorphology can improve our understanding of

the shaping of landscapes (Corenblit et al., 2011). Some examples illustrate that even the simplest aspects of some systems cannot be understood without considering the biogeomorphological coupling (Murray et al., 2008). Murray et al. (2008) stated that the influences of biology on sediment transport and morphological change are relatively easy to recognize and measure. However, the change of organisms to the evolution of the landscape is less obvious.

In order to make progress into the understanding of the dynamics of landscapes, it is very important to seek for a two-way coupling in biomorphodynamic feedbacks according to Murray et al. (2008). Corenblit et al. (2011) suggest some directions for future investigations. First of all the improvement of biogeomorphological conceptual models. Secondly, the identification of engineer species that create landforms. Thirdly, the organization of field studies to quantify the effects of engineer species. And finally, the development of numerical models for simulating and analyzing biogeomorphological feedbacks.

Up to now, some explorations on the biological activity in sand waves have already been done. The potential impact of ecosystem engineering species (creates, maintains or modifies habitats (Jones et al., 1994)) on the migration rate, dimensions, and occurrence of tidal sand waves is demonstrated by Borsje et al. (2009a), Borsje et al. (2009b), and Borsje et al. (2009c). Borsje et al. (2009c) proposed a parameterization of three ecosystem engineering species. By including these species into the model, the occurrence of tidal sand waves was significantly better predicted. Furthermore, Borsje et al. (2008) found out that *Lanice conchilega* causes the sand wave length to decrease, due to the reduction of the near-bottom flow. This was in agreement with field studies. The main initiator for the better prediction of occurrence of sand waves and sand wave length was the sand mason worm *Lanice conchilega*. This ecosystem engineering species lives in significant amounts at the bed-water interface of the bottom of the North Sea. Furthermore, a lot of studies have been done to the species *Lanice conchilega*, for example field and flume studies, but also model studies. Therefore, it is possible to compare model results with field observations.

For all of these studies a linear model has been used which only shows the initial growth and sand wave length. Furthermore, only a one-way coupling was included in the model, which solely consisted of the effects on the morphodynamics due to the presence of *Lanice conchilega*. They did not include the feedback from the morphodynamics on the distribution of the ecosystem engineering species. Using a non-linear model, more characteristics of sand waves can be investigated and it is possible to include a two-way coupling.

Borsje (2012) made a first exploration to include a two-way coupling into a sand wave model. However, this was only a draft, and it should be extended. In this study, the model of Borsje (2012) is elaborated. For example the method, of adapting the density of *Lanice conchilega* to every season is improved by a growth factor. With this model, we will show that a two-way coupling is important to give a good estimation of sand wave growth.

1.2 Research objective

Based on the problem definition, the main objective of this research is stated as follows:

*To determine the effects of a two-way coupling between dynamic patches of *Lanice conchilega* and dynamically active sand waves, by using the process-based model Delft3D.*

The research questions follow from the research objective. They are defined as follows:

1. What is the influence of patches of *Lanice conchilega* on the sediment transport rates on a flat bed for varying tube densities, tube lengths and patch sizes?
2. How can the distribution of patches of *Lanice conchilega* be explained by the physical conditions along the sand waves crest, trough, and flank?
3. What is the influence of the interaction between dynamic patches of *Lanice conchilega* and sand wave dynamics on the growth of sand waves?

1.3 Method

This work is based on the model of Borsje (2012) and later on the work of Van Gerwen et al. (2016). The sand mason worm *Lanice conchilega* is implemented in a 2DV model in order to determine the influence on the local hydrodynamics and sediment dynamics, therefore the process-based model Delft3D is used. Three different model set-ups are applied to investigate the effects of *Lanice conchilega*. The first model set-up has a flat bottom and a static tube density. The second model set-up has a sinusoidal bottom and the density of the tubes differs every season. On this bottom the two-way coupling of dynamic patches of *Lanice conchilega* and sand waves are studied. The third and last model set-up has a self-organizational bottom as well as a dynamic tube density.

Figure 1.2 consists of a flow chart in which the one-way and two-way coupling between the community *Lanice conchilega* and landforms is shown. The Delft3D model set-up, used for the modulation of the landform by the community, is explained in detail in chapter 3. How the community is selected by the sand waves (RQ2) is explained in chapter 2 (sec. 2.3). The inclusion of the biological activity into the modeling is described in detail in chapter 4. The corresponding chapters and research questions belonging to the specific parts are mentioned in the figure.

1.4 Outline

Chapter 2 This chapter describes the sand mason worm *Lanice conchilega*. Its characteristics, life cycle, and habitat are discussed, as well as some field studies. A physical description of the effects of the tubes on the hydrodynamics and sediment dynamics is included.

Chapter 3 Delft3D is the model used to investigate the effects of *Lanice conchilega* on landforms, the model set-up is explained in this chapter.

Chapter 4 The implementation of dynamic patches of *Lanice conchilega* into the sand wave model is explained as well as the assumptions made for the implementation.

Chapter 5 This chapter describes the effects of *Lanice conchilega* on the hydrodynamics and morphodynamics on a flat bottom.

Chapter 6 The two-way coupling of *Lanice conchilega* and sinusoidal sand waves and self-organisational sand waves is discussed here.

Chapter 7 The discussion of the method and the results is presented here.

Chapter 8 This chapter contains the conclusions and recommendations of the research.

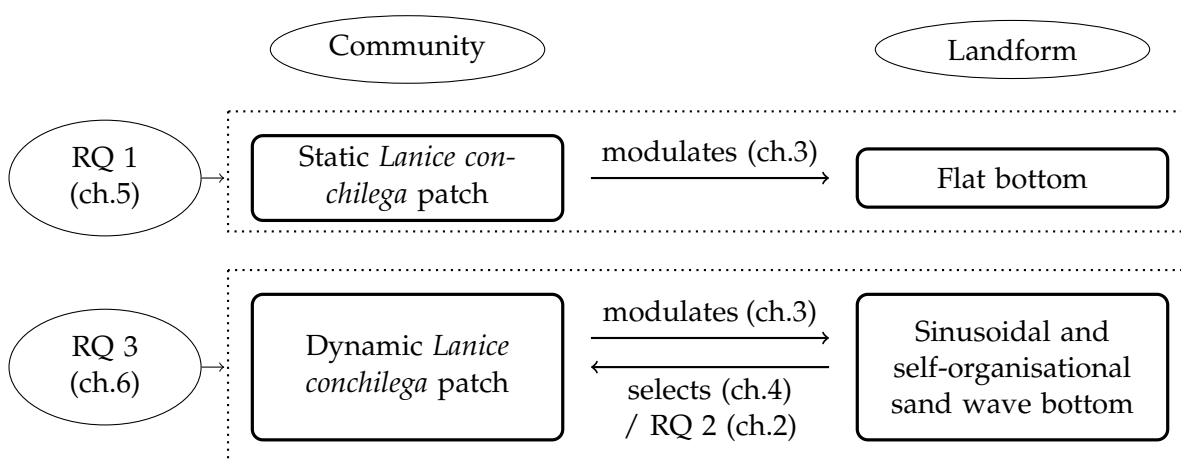


FIGURE 1.2: Flow chart of the interaction between the community *Lanice conchilega* and landforms. The corresponding chapters (ch.) and research questions (RQ) are mentioned. Adapted after Corenblit et al. (2011).

CHAPTER 2

Characteristics of *Lanice conchilega*

Macrozoobenthics are animals living at the sea bed, which are visible with the naked eye. *Lanice conchilega* is one of these animals, which is specifically living at the bed-water interface. Furthermore, *Lanice conchilega* can be specified as an ecosystem engineer (Jones et al., 1994). Ecosystem engineers maintain, modify or create habitats both in a direct and indirect way. The following sections provide an overview of this animal. Section 2.1 gives a short introduction about *Lanice conchilega*. Section 2.2 shows its life cycle. Section 2.3 explains the preferred habitat. Section 2.4 describes some field studies about *Lanice conchilega*. Finally, section 2.5 describes the effects of *Lanice conchilega* on the hydrodynamics and sediment dynamics.

2.1 Introduction

The tube building polychaete *Lanice conchilega* is a sand mason worm and it consists of three important parts, the worm itself, the tube, and the fringe (fig. 2.1A). The length of the worm can be up to 65 cm and its diameter is around 0.5 cm. The inner thin organic layer of the worm, is attached to a tube of sand or shell breccia (Ziegelmeier, 1952). The tube protrudes approximately 1 to 4 cm from the sediment into the water column. It is crowned with a sand fringe, which is used for feeding. Furthermore, the worm lives in colonies which are called patches (fig. 2.1C). When *Lanice conchilega* occurs in low densities in these patches, the worm prefers surface deposit feeding, however it switches to suspension feeding in case of high densities (Buhr, 1976). The worms are found on all coasts of Europe and in both the Atlantic and the Pacific, but it is absent from arctic waters (Holthe, 1978).

Lanice conchilega has a high ecological importance. For example, the sediment properties (Jones and Jago, 1993) and the oxygen transport (Forster and Graf, 1995) are affected. Secondly, the composition of the benthic communities is altered (Zühlike, 2001). And finally, it is an important food item for fish and birds (Petersen and Exo, 1999).

2.2 Life cycle

The worm of *Lanice conchilega* has a complex life cycle, and it consist mainly of three phases. The larval phase, juvenile phase and adult phase.

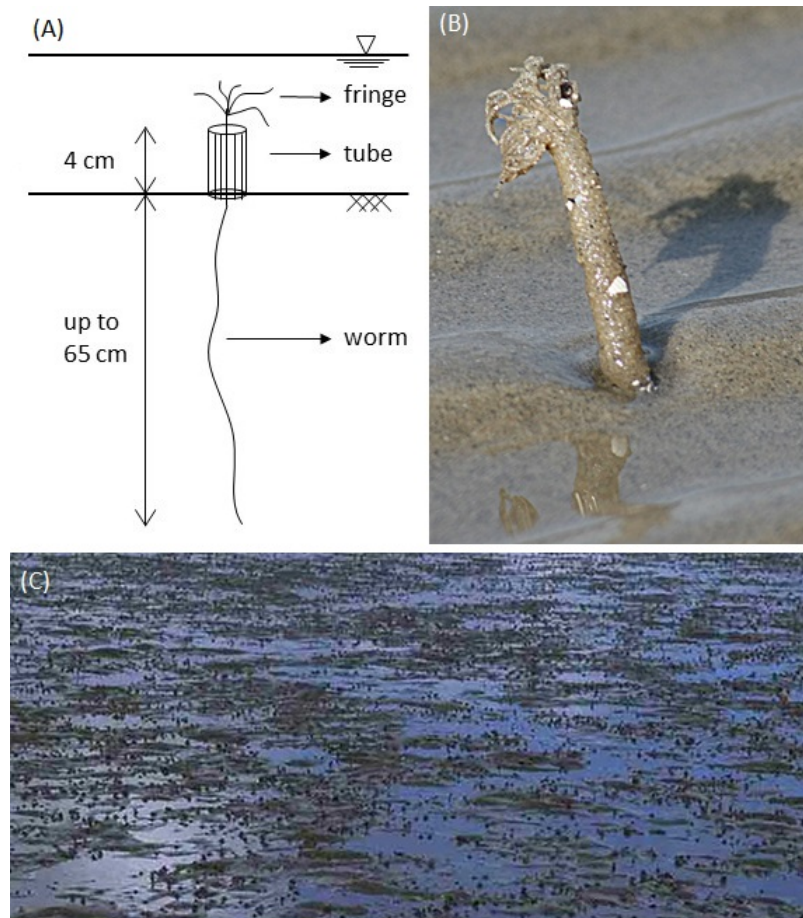


FIGURE 2.1: (A) A schematization of an individual, showing the worm, tube and fringe. (B) An individual of *Lanice conchilega*. (C) A patch of *Lanice conchilega*.

The larval phase is characterized by the presence of a transparent tube, which is used as a floating device (Bhaud and Cazaux, 1990). This phase is also termed 'aulophore' by Kessler (1963). The aulophore larvae looks like a juvenile individual endowed with larval characteristics, these larval characteristics persist until they settle (Bhaud, 2000). The larvae prefer to settle to an adult tube (Carey, 1987; Heuers et al., 1998), however other research indicates that larvae also attach to other substratum (Heuers and Jaklin, 1999; Strasser and Pieloth, 2001). During the settlement, the tentacles or the aulophore larvae play an important role. The anterior end of the larval tube is glued to the preferred substratum. The length and width of the tube is extended by gathering sediment particles (Heimler, 1981).

On average 5-13 juveniles attach to one adult tube. Approximately one month after settlement at an adult tube, the juveniles detach, and settle in close proximity to the adults (Callaway, 2003). After detaching the individual grows and stabilizes itself into the sediment. The capability of re-establishing its tube after being washed out remains (Nicolaidou, 2003), however it does not always happen. The life-span of the worm can be 1-2 years (Beukema et al., 1978) or can be up to 3 years (Ropert and Dauvin, 2000).

The recruitment of *Lanice conchilega* occurs in three seasons. These periods are defined based on the occurrence of peaks of aulophore larvae in the water column.

The three seasons are: spring, summer and autumn; whereas spring shows the highest recruitment (Van Hoey, 2006). The recruitment of *Lanice conchilega* only occurs within a patch, because the juveniles are directly attached to an adult (Heuers et al., 1998).

2.3 Habitat

The distribution of macrozoobenthic communities in the North Sea is correlated to environmental variables. For example, it is highly correlated to characteristics of the sediment type, such as grain size, mud content and organic content. Other correlations occur with water temperature, water depth and latitude (De Jong et al., 2015). Depending on these and other parameters, species will settle at a certain location.

An important parameter to predict the occurrence of *Lanice conchilega* is the % mud content (Willems et al., 2008). Furthermore, Herman et al. (2001) showed that the bed shear stress can affect macrozoobenthos. First of all, the biomass of suspension feeders was highest where the bed shear stress was minimal. They concluded that muddy situations are present where the bed shear stress is low. Also holds that where the bed shear stress is low, the sediment is muddy. Moreover, De Jong et al. (2015) concluded that apart from sediment variables, the bed shear stress can explain distribution of macrozoobenthos along sand waves. A low mean bed shear stress causes a higher macrozoobenthic species richness.

Van Dijk et al. (2012) presented the spreading of marine habitats over tidal sand ridges. At the well-sorted crests, the communities were low in density and diversity. At the poorly sorted, muddy troughs, the communities were high in density and diversity. This sorting pattern is present in sand waves as well. Roos et al. (2007) showed that a general trend is seen of coarser and well-sorted sediments at the sand wave crests and finer-grained and less well-sorted sediments in the troughs.

These findings suggests that patches of *Lanice conchilega* will settle at troughs and lower flanks of sand waves, where bed shear stress is low and mud is available.

Rabaut et al. (2009) classified *Lanice conchilega* as reefs in the intertidal system. The classifications of reefs are present in the mounds with *Lanice conchilega*, namely elevation, sediment consolidation, spatial extent, patchiness, reef builder density, biodiversity and community structure are significantly altered. Furthermore, the reefs should be stable enough to persist for several years. This research suggest furthermore that subtidal systems are expected to be more stable than intertidal systems. On the other hand, Strasser and Pieloth (2001) showed that after severe winters high mortality rates are present. The patch fully recovered three years after the destruction.

2.4 Field studies

The species *Lanice conchilega* occurs in the intertidal and subtidal zone. Many field studies have been done in the intertidal zone, less studies have been done in the subtidal zone. The topic of interest for this study is the subtidal zone, therefore some subtidal field studies are explained here. Because there is a lot more information available about the intertidal zone, also some intertidal studies are explained.

Degraer et al. (2008) evaluated *Lanice conchilega* to be classified as a reef or not. Therefore very high resolution side-scan sonar mapping has been used. In the subtidal area the patches had a varying density between 0 and 1979 $ind.m^{-2}$. The size of the patch had a maximum of 15 m^2 . However the mound height of the patch could not be determined. In the intertidal area the densities were much higher, on average it was $2813 \pm 880 ind.m^{-2}$. The reefs covered about 10% of the area and the mound height was between 7.5 cm and 11.5 cm.

Van Hoey et al. (2008) evaluated the presence of *Lanice conchilega* in different habitats in the North Sea. It has a low habitat specialization, but it mainly occurs in sandy sediments, from mud to coarse sand. Shallow muddy sands were strongly preferred. In muddy sands the densities were more than 1000 $ind.m^{-2}$ compared to a maximum of 575 $ind.m^{-2}$ in shallow medium sands. Van Hoey et al. (2006) mentioned that patches rose between 10 and 40 cm from the sea bed, in both subtidal and intertidal areas.

De Jong et al. (2015) studied macrozoobenthic distribution patterns in the Dutch coastal subtidal zone. *Lanice conchilega* was found where the bed shear stress was low. The density found was up to 985 $ind.m^{-2}$.

Table 2.1 shows a summary of the field studies.

2.5 Effects of tubes on hydrodynamics and sediment dynamics

The tubes of the *Lanice conchilega* worm affect the local water currents and change the sedimentary processes. These processes are described below.

Figure 2.2A shows the water flow over a flat bottom. In this idealized situation without interruptions, the water flow has few turbulence and therefore low Reynolds stresses. Due to friction with the bottom, the near-bed flow velocity is smaller than the flow velocity higher up into the water column.

Figure 2.2B shows the same flat bottom, however in this situation a patch with tubes of *Lanice conchilega* is located in the middle of the domain. The water flow becomes disturbed and it flows trough and over the patch. First of all, due to the protruding tubes from the sediment, the bed roughness becomes higher compared to the surrounding area. The higher roughness causes lower near-bed velocities compared to the original situation without patch (Friedrichs et al., 2000). The lower near-bed velocities within the patch, facilitates fine sediment to deposit (Borsje et al., 2014a). Mounds are formed by the deposition of sediment between the tubes (fig. 2.2C).

Furthermore, Friedrichs et al. (2000) has shown that above the patch, a 'skimming flow' arises. In this situation objects protruding from the sediment hinder the water flow, and the main flow is going over the objects instead of through the objects. In this case the sediment is not eroded from the bed.

Dependent on the density of the tubes, the patch will form a barrier for the water flow. For larger densities, less water can flow through the patch, and the barrier effect will be larger. The height of this barrier is dependent on the length of the tubes and the mound height.

The sediment transport is largely determined by the hydrodynamic conditions. Turbulence is able to lift sediment particles and if the lift force is large enough, the particles are brought into suspension. The suspended sediment is distributed over the whole water column due to turbulence. This effect is caused by bottom friction

and differences in velocity between two adjacent horizontal water layers. However, within a patch the near-bed velocities and turbulence becomes very low, such that the sediment deposits between the tubes.

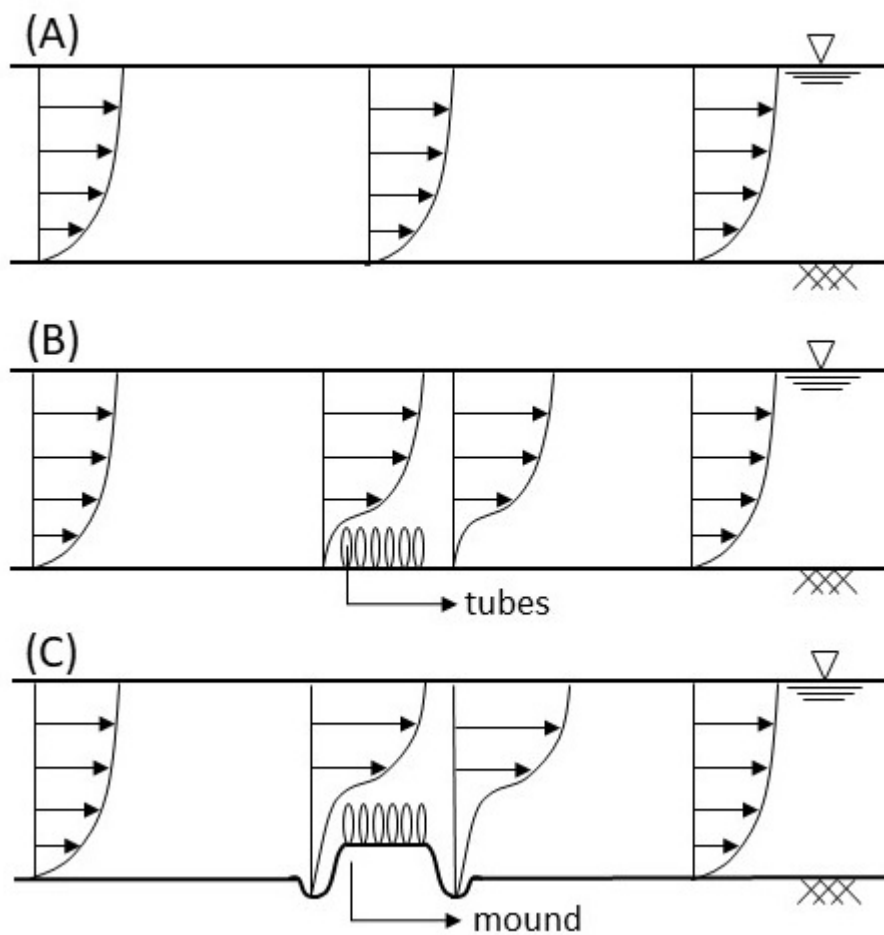


FIGURE 2.2: Schematization of velocity profiles above: (A) an undisturbed bottom, (B) a flat bottom with patch, (C) a mound with *Lanice conchilega* after sediment has been trapped between the tubes. The arrows indicate the horizontal velocities.

Reference \ Characteristic	subtidal / intertidal	Tube density [<i>ind.m</i> ⁻²]	Size patch [<i>m</i> ²]	Mound height [cm]	Covering [%]
Degraer et al. (2008)	subtidal	Up to 1979	15	-	-
Degraer et al. (2008)	intertidal	2813 ± 880	-	7,5 to 11,5	10
Van Hoey et al. (2008)	subtidal	Maximum: 5000	-	-	-
Rabaut (2009)	intertidal	Average: 3259	1 to 12	Average: 8,4	18,4
De Jong et al. (2015)	subtidal	Maximum: 8262	Average: 1.37	Maximum: 16,5	-
		Up to 985	-	-	-

TABLE 2.1 : Characteristics of *Lanice conchilega* found in different field studies

 CHAPTER 3

Model set-up

This chapter explains the model set-up used for this research. Section 3.1 describes the hydrodynamic and transport equations used in Delft3D. Section 3.2 shows the vegetation model used to model the tubes of *Lanice conchilega*. Section 3.3 shows the grids used for the three cases.

3.1 Delft3D

The numerical shallow water model Delft3D has been used to model the ecosystem engineer *Lanice conchilega* on flat bottoms and sand waves. The equations used in this model are horizontal momentum equations, a continuity equation, a turbulence closure model, a sediment transport equation and a sediment continuity equation (Lesser et al., 2004). Vertical accelerations are assumed to be small compared to gravitational acceleration, so the vertical momentum equation is reduced to the hydrostatic pressure relation. A sigma layering has been applied in the vertical in order to solve the model equations. The model is run in 2DV mode, which means that the flow is considered in x and z direction only. In the z direction, zero flow is assumed and the Coriolis effects are ignored. Coriolis effects have been shown to have negligible effects at the length of sand waves (Hulscher, 1996). Section 3.1.1 describes the hydrodynamic equations and section 3.1.2 explains the transport equations.

3.1.1 Hydrodynamic equations

The horizontal momentum equations is as follows:

$$\frac{\partial u}{\partial t} + u \frac{\partial u}{\partial x} + \frac{\omega}{(H + \zeta)} \frac{\partial u}{\partial \sigma} = -\frac{1}{\rho \omega} P_u + F_u + \frac{1}{(H + \zeta)^2} \frac{\partial}{\partial \sigma} \left(\nu \frac{\partial v}{\partial \sigma} \right). \quad (3.1)$$

The continuity equation is as follows:

$$\frac{\partial \omega}{\partial \sigma} = -\frac{\partial \zeta}{\partial t} - \frac{\partial [(H + \zeta)u]}{\partial x}, \quad (3.2)$$

where:

- u [ms^{-1}] horizontal velocity in x direction,
- ω [s^{-1}] vertical velocity relative to the moving vertical $\sigma - plane$,

H	[m]	water depth,
ζ	[m]	free surface elevation,
ρ_w	[kgm ⁻³]	water density,
P_u	[Nm ⁻²]	pressure gradient,
E_u	[ms ⁻²]	horizontal Reynold's stresses,
ν	[m ² s ⁻¹]	kinematic viscosity.

The $k - \epsilon$ turbulence closure model is used for the vertical eddy viscosity, in which the turbulent energy k and the dissipation ϵ are calculated (Burchard et al., 2008):

$$\nu = c_\mu \frac{k^2}{\epsilon}, \quad (3.3)$$

where:

c_μ	[-]	constant with a recommended value of 0.09 (Rodi, 1984),
k	[m ² s ⁻²]	turbulent kinetic energy,
ϵ	[m ² s ⁻³]	turbulet energy dissipation.

At the bed ($\sigma = -1$), the vertical velocity ω is set to zero and a quadratic friction law is applied:

$$\tau_b \equiv \rho_w \frac{\nu}{(H + \zeta)} \frac{\partial u}{\partial \sigma} = \rho_w u_* |u_*|, \quad \omega = 0, \quad (3.4)$$

where:

τ_b	[Nm ⁻²]	bed shear stress,
u_*	[ms ⁻¹]	shear velocity that relates the velocity gradient at the bed to the velocity u in the lowest computational grid point by assuming a logarithmic velocity profile.

At the free surface ($\sigma = 0$), the vertical velocity ω is set to zero and a no-stress condition is applied:

$$\rho_w \frac{\nu}{(H + \zeta)} \frac{\partial u}{\partial \sigma} = 0, \quad \omega = 0. \quad (3.5)$$

3.1.2 Sediment transport and bed evolution equations

The suspended sediment transport is calculated by solving the advection-diffusion equation:

$$\frac{\partial c}{\partial t} + \frac{\partial(cu)}{\partial x} + \frac{\partial(w - w_s)c}{\partial z} = \frac{\partial}{\partial x} \left(\epsilon_{s,x} \frac{\partial c}{\partial x} \right) + \frac{\partial}{\partial z} \left(\epsilon_{s,z} \frac{\partial c}{\partial z} \right), \quad (3.6)$$

where:

c	[kgm ⁻³]	mass concentration of sediment,
$\epsilon_{s,x}, \epsilon_{s,z}$	[m ² s ⁻¹]	sediment diffusivity coefficients in x and z direction.

All sediment above the reference height $a = 0.01H$ is included as suspended sediment. The reference concentration, c_a at height a is given by (Van Rijn, 2007):

$$c_a = 0.015\rho_s \frac{dT_a^{1.5}}{aD_*^{0.3}}. \quad (3.7)$$

T_a is the non-dimensional bed shear stress:

$$T_a = \frac{u_c \tau_b - \tau_{cr}}{\tau_{cr}}, \quad (3.8)$$

where:

u_c	[-]	efficiency factor, ratio between the grain related friction factor and the total current related friction factor,
τ_{cr}	[Nm^{-2}]	critical bed shear stress for the initiation of motion of sediment,
D_*	[-]	non-dimensional particle diameter,
ρ_s	[kgm^{-3}]	specific density of the sediment.

The bed load transport is calculated by (Van Rijn et al., 2004):

$$S_b = 0.006\alpha_s\rho_s\omega_s dM^{0.5}M_e^{0.7}, \quad (3.9)$$

where:

α_s	[-]	correction parameter of the slope effects,
ω_s	[$m s^{-1}$]	settling velocity of the sediment,
d	[m]	sediment grain size,
M	[-]	sediment mobility number,
M_e	[-]	excess sediment mobility number.

M and M_e , the sediment mobility number and excess sediment mobility number, are given by:

$$M = \frac{u_r^2}{(\rho_s/\rho_w - 1)gd}, \quad (3.10)$$

$$M_e = \frac{(u_r - u_{cr})^2}{(\rho_s/\rho_w - 1)gd}, \quad (3.11)$$

where:

u_r	[ms^{-1}]	magnitude of the equivalent depth-averaged velocity computed from the velocity in the bottom computational layer assuming a logarithmic velocity profile,
u_{cr}	[ms^{-1}]	critical depth-averaged velocity for the initiation of motion of sediment based on the shields curve.

Bed level gradients affect the bed load transport, this means that sediment is transported more easily downhill than uphill. The correction parameter α_s is given by (Bagnold, 1956):

$$\alpha_s = \lambda_s, \quad (3.12)$$

where:

λ_s [-] slope parameter, which is usually taken inversely proportional to the tangent of the angle of repose of sand (Sekine and Parker, 1992) leading to $\lambda_s = 2.5$.

The Exner equation is used to calculate the bed evolution:

$$(1 - \epsilon_p) \frac{\partial z_b}{\partial t} + \frac{\partial(S_b + S_s)}{\partial x} = 0, \quad (3.13)$$

$$\int_a^{(H+\zeta)} \left(uc - \epsilon_{s,z} \frac{\partial c}{\partial x} \right) dz, \quad (3.14)$$

where:

z_b [m] upwards positively defined bed level,
 ϵ_p [-] bed porosity with value 0.4,
 S_b [$kgm^{-1}s^{-1}$] bed load transport (eq. 3.9),
 S_s [$kgm^{-1}s^{-1}$] suspended load transport (eq. 3.14).

3.2 Vegetation model

The tubes of the *Lanice conchilega* worm are influencing the near-bottom flow, as explained in section 2.5. The logarithmic velocity profile is deviated due to the protruding tubes (Borsje et al., 2014a). In order to include this effect into the model, the tube building worms are represented as thin, solid piles on the bottom of the seabed. These piles are included with the vegetation model of Delft3D, the turbulent flow over and through the vegetation is calculated with this model (Uittenbogaard, 2003). The input parameters for this model is the plant geometry, such as the diameter, density, height and drag coefficient. The effect of cylinders on the flow velocity is taken into account by this model (fig. 2.2).

The influence of cylindrical structures on drag is accounted for by an extra source term of friction force in the momentum equation. The momentum equation is stated as follows (Uittenbogaard, 2003):

$$\rho_w \frac{\partial u(z)}{\partial t} + \frac{\partial p}{\partial x} = \frac{\rho_w}{1 - A_p(z)} \frac{\partial}{\partial z} \left\{ (1 - A_p(z)) (\nu + \nu_T(z)) \frac{\partial u(z)}{\partial z} \right\} - \frac{F_r(z)}{1 - A_p(z)}, \quad (3.15)$$

$$A_p(z) = \frac{1}{4} \pi D_{cyl}(z)^2 n(z), \quad (3.16)$$

$$F_r(z) = \frac{1}{2} \rho_w C_D a(z) |u(z)| u(z), \quad (3.17)$$

$$a(z) = d(z) n(z), \quad (3.18)$$

where:

$\frac{\partial p}{\partial x}$	$[kgm^{-2}s^{-2}]$	horizontal pressure gradient,
A_p	[-]	solidity of the vegetation measured on a horizontal cross section at vertical level z ,
ν_T	$[m^2s^{-1}]$	eddy viscosity,
F_r	$[Nm^{-3}]$	resistance force,
D_{cyl}	$[m]$	diameter of the cylindrical structure,
n	$[m^{-2}]$	number of cylinders per unit area.

The influence of the cylinders on the turbulence is included by an extra source term of Total Kinetic Energy (TKE) (Temmerman et al., 2005):

$$\left(\frac{\partial k}{\partial t}\right)_{cylinders} = \frac{1}{1 - A_p(z)} \frac{\partial}{\partial z} \left\{ (1 - A_p(z)) (\nu + \nu_T / \sigma_k) \frac{\partial k}{\partial z} \right\} + T(z), \quad (3.19)$$

$$T(z) = F_r(z)u(z)/\rho_w, \quad (3.20)$$

where:

k	$[m^2s^{-2}]$	turbulent kinetic energy,
T	$[m^2s^{-2}]$	work spent by the fluid.

The influence of the cylinders on the turbulence is also included by an extra source term of of turbulent energy dissipation (Temmerman et al., 2005):

$$\left(\frac{\partial k}{\partial t}\right)_{cylinders} = \frac{1}{1 - A_p(z)} \frac{\partial}{\partial z} \left\{ (1 - A_p(z)) (\nu + \nu_T / \sigma_k) \frac{\partial k}{\partial z} \right\} + T(z)\tau_\epsilon^{-1}, \quad (3.21)$$

where:

ϵ	$[m^2s^{-2}]$	turbulent energy dissipation,
τ_ϵ	[-]	minimum of τ_{free} or $\tau_{cylinders}$,

$$\tau_{free} = \frac{1}{c_{2\epsilon}} \left(\frac{k}{\epsilon}\right), \quad (3.22)$$

$$\tau_{cylinders} = \frac{1}{c_{2\epsilon}\sqrt{c_\mu}} \left(\frac{L^2}{T}\right)^{1/3}, \quad (3.23)$$

$$L(z) = C_l \left\{ \frac{1 - A_p(z)}{n(z)} \right\}^{1/2}, \quad (3.24)$$

where:

$c_{2\epsilon}$	[-]	coefficient,
c_μ	[-]	coefficient,
C_l	[-]	coefficient reducing the geometrical length scale.

3.3 Grid

Two model set-ups are used, one for the flat bottom, and one for the sand wave bottom. The following subsections describe the grid of these two model set-ups.

3.3.1 Flat bottom

The flat bottom case is run in 2DV. The model domain is 1000 meters. The middle of the domain consists of 200 cells with a width of 0.5 meter. The width of the grid cells is increasing to the end of the boundary to 30 meters. In total there are 258 grid cells (fig. 3.1). The vertical orientation is composed of 100 layers, with small vertical steps near the bed and increasing steps towards the water surface. At the lateral boundary, a Riemann boundary is imposed, which allows the waves to cross the open boundaries without being reflected into the computational domain.

3.3.2 Sinusoidal bottom

The sand wave bottom case is also run in 2DV. The model domain is 48 kilometers, also with a variable horizontal resolution. The middle of the domain has 1000 grid cells with a width of 2 m with increasing width until approximately 1500 m towards the boundaries. In total there are 1058 horizontal grid cells (fig. 3.2). The vertical layering consists of 60 layers, a small width at the bottom and increasing width towards the water surface. At the boundaries Riemann boundaries are imposed, which allow the waves to cross the open boundaries without being reflected into the computational domain.

TABLE 3.1: Grid parameters of two set-ups

	Flat bottom	Sand wave bottom
Total horizontal domain [km]	1	48
Amount of small grid cells	200	1000
Grid cell width [m]	0.5	2
Amount of vertical layers	100	60
Boundaries	Riemann	Riemann

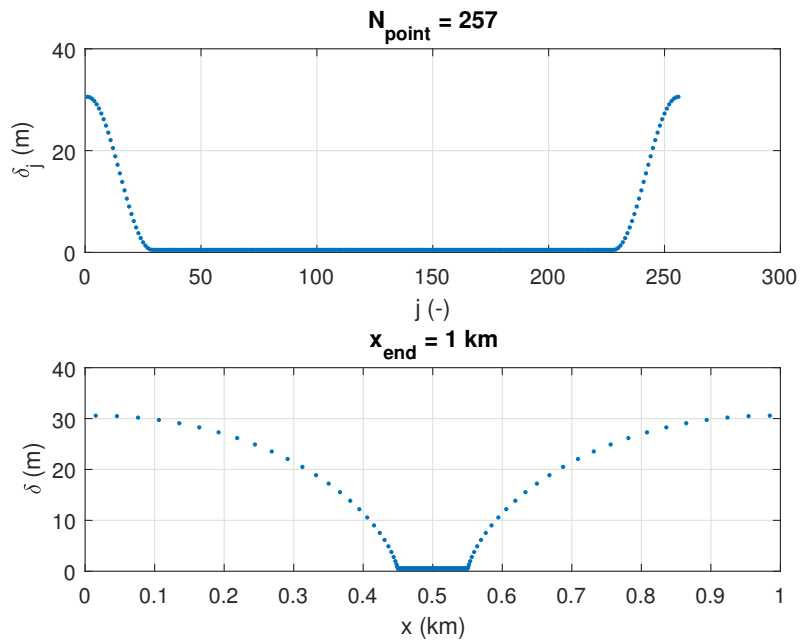


FIGURE 3.1: Division of horizontal grid cells for the flat bottom set-up

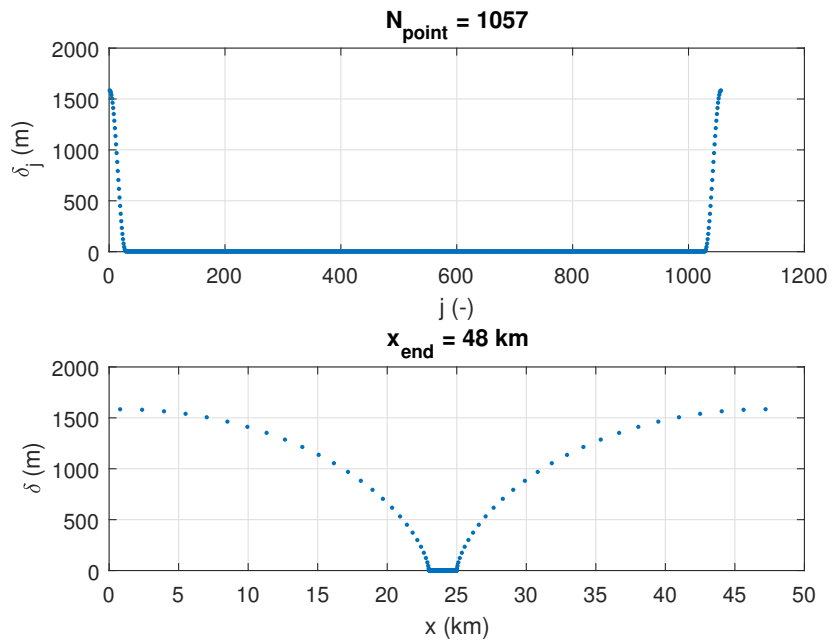


FIGURE 3.2: Division of horizontal grid cells for the sand wave bottom set-up

 CHAPTER 4

Inclusion of biological activity

This chapter describes the implementation of *Lanice conchilega* into the sand wave model. Section 4.1 explains the growth factors used for tube density and bottom covering. Section 4.2 explains the assumptions made to implement *Lanice conchilega* into the sand wave model. And finally, section 4.3 explains the model used to describe the tube density and bottom covering.

4.1 Growth factors

Growth factors are used for the growth in tube density and bottom covering. Section 4.1.1 explains the factors for the tube density growth and section 4.1.2 explains the growth in bottom covering.

4.1.1 Tube density growth

The growth in tube density depends on two processes (eq. 4.1). First of all, the recruitment within a patch, and secondly, the available suspended sediment as food for the worms. A recruitment factor (R) and a sediment factor (S), respectively, are used to determine the density of the tubes in the next season.

$$\text{Tube density growth factor} = R(D) * S(\langle c \rangle) \quad (4.1)$$

These two factors are stated as autonomous factors, however they are correlated to each other. The density of the previous season is used to calculate the next density, however the sediment factor is already included in the density of the previous season. In order to show how these factors are calculated and to find out which of the two sediment factors is the most realistic one, these factors are dealt with separately.

Recruitment factor

A logistic growth curve, analogous to the method of Crouzy et al. (2016) and Bärenbold et al. (2016), is used to determine the recruitment factor of *Lanice conchilega*. Figure 4.1 shows the logistic growth curve. It can be interpreted as follows, at the start the density increases slowly, because the amount of individuals is low. At the end the density increases slowly as well, but now because the patch size is the restricting factor. There is not more space for more tubes. At half of the maximum density the increase is largest, because all factors are most optimal. The factors are

the availability of food, the area and the amount of individuals. The Ordinary Differential Equation (ODE) which describes the behavior of logistic growth in figure 4.1 is shown in equation 4.2. The solution of this ODE is shown in equation 4.3.

$$\frac{\partial D}{\partial t} = \alpha_g * D(t) * (D_{max} - D(t)), \quad (4.2)$$

$$D(t) = D_0 \frac{D_{max}}{D_0 + e^{-D_{max}\alpha_g t}(D_{max} - D_0)} = D_0 * R(D), \quad (4.3)$$

where:

$D(t)$	[ind. m^{-2}]	tube density at a specific moment in time,
D_0	[ind. m^{-2}]	initial density of <i>Lanice conchilega</i> ,
D_{max}	[ind. m^{-2}]	maximum density of <i>Lanice conchilega</i> ,
α_g	[$m^2 \text{ ind.}^{-1} \text{ seasons}^{-1}$]	growth factor,
t	[seasons]	time,
$R(D)$	[-]	recruitment factor dependent on density in previous season.

The recruitment factor is deduced from the derivative (eq. 4.3). It is used in step two, three and five of the method described in section 4.3.

Figure 4.1 shows the growth in tube density. The first assumption for this graph is that the patch is full-grown with tubes after one year, without considering if there is enough food available. The second assumption is that the maximum density is 300 or 800 $ind.m^{-2}$. These two assumptions lead to the growth factors α_g .

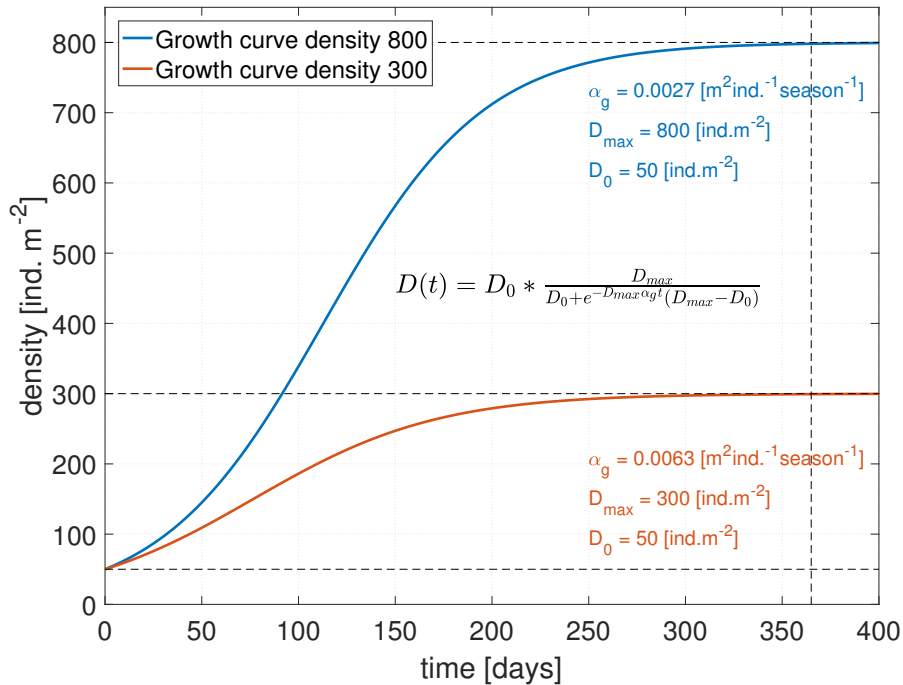


FIGURE 4.1: Growth-curve for tube density. The horizontal upper dotted line shows where the patch its full density for 800 $ind.m^{-2}$. The middle dotted line represents the maximum density of 300 $ind.m^{-2}$. The lower dotted line shows the minimum density. The vertical dotted line shows when the maximum is reached.

Sediment factor

The growth in tube density is also dependent on the suspended sediment available in the system. This is a measure for the available food. This factor can be calculated in two ways. The first option is to divide the tide-averaged suspended sediment concentration at the location of the patch by the maximum suspended sediment concentration in the whole system (eq. 4.4). The second option is to divide the tide-averaged suspended concentration at the location of the patch by the mean tide-averaged suspended sediment concentration in the whole system and this value is restricted by 0.4 and 1 (eq. 4.5). One of these two sediment factors is used in step two, three and five of the method described in section 4.3. The difference between these two factors is tested later on. The two factors are:

$$S(\langle c \rangle) = \frac{\langle c \rangle}{\max\langle c \rangle}, \quad (4.4)$$

$$S(\langle c \rangle) = \frac{\langle c \rangle}{\text{mean}\langle c \rangle} \quad \text{for } 0.4 < S < 1, \quad (4.5)$$

where:

$S(\langle c \rangle)$	[-]	sediment factor dependent on the sediment concentration at the specific location of the patch,
$\langle c \rangle$	$[kg\ m^{-3}]$	tide-averaged suspended sediment concentration,
$\max\langle c \rangle$	$[kg\ m^{-3}]$	maximum tide-averaged suspended sediment concentration,
$\text{mean}\langle c \rangle$	$[kg\ m^{-3}]$	mean tide-averaged suspended sediment concentration in whole domain.

4.1.2 Bottom covering growth

Also for the growth in bottom covering with patches, a logistic growth curve has been used (fig. 4.2). The ODE and the solution of the problem are:

$$\frac{\partial C}{\partial t} = \beta_g * C(t) * (C_{max} - C(t)), \quad (4.6)$$

$$C(t) = C_0 \frac{C_{max}}{C_0 + e^{-C_{max}\beta_g t}(C_{max} - C_0)} = C_0 * B(C), \quad (4.7)$$

where:

$C(t)$	[%]	covering at a specific moment in time,
C_0	[%]	initial covering of the bottom,
C_{max}	[%]	maximum covering of the bottom,
β_g	$[\%^{-1}\ \text{years}^{-1}]$	growth factor,
t	[years]	time,
$B(C)$	[-]	seeding factor dependent on covering of previous season.

The solution of the ODE is used as a factor representing the seeding of patches on the bottom. This factor is used in step five of the method.

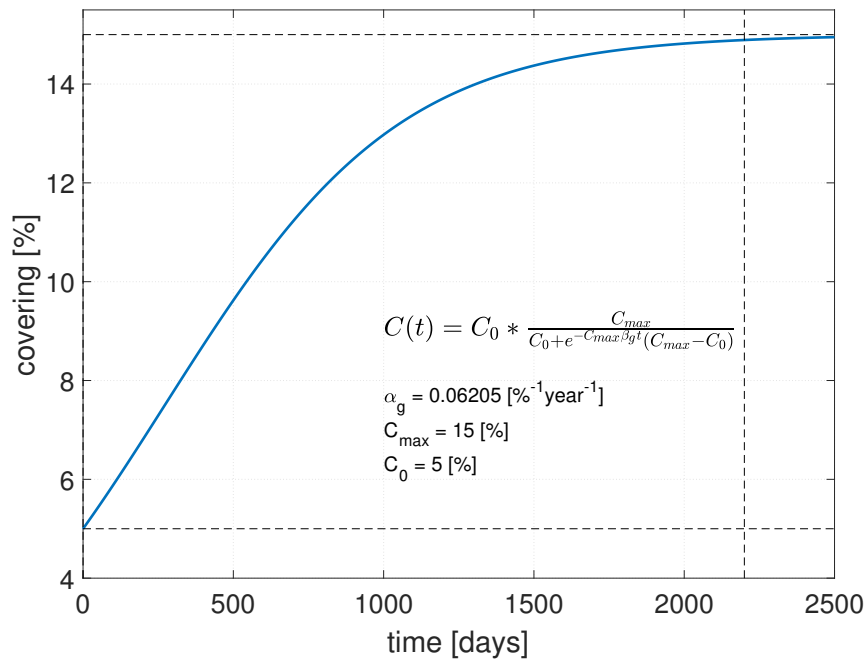


FIGURE 4.2: Growth-curve for bottom covering. The upper dotted line shows the maximum covering, the lower dotted line the minimum and the vertical dotted line shows when the maximum is reached.

4.2 Assumptions

In order to describe the variation of *Lanice conchilega* into the sand wave model, the following assumptions are made concerning chapter 2 and 3.

- Field observations show that there are three recruitment periods (spring, summer and autumn) (Van Hoey et al., 2006). Therefore in these three seasons the density will be updated. The recruitment only takes place within a patch.
- Every five years all patches fully disappear (Strasser and Pieloth, 2001). Every year only a certain percentage of the tubes within the patch disappears, because patches can be classified as reefs (Rabaut et al., 2009).
- The recruitment factor is depending on the available suspended sediment concentration. Since *Lanice conchilega* is a filter-feeder, suspended sediment is used as food (Buhr, 1976).
- Only the tube of the worm which protrudes from the sediment has an influence on the hydro- and morphodynamics. Therefore, only the tube is modeled.
- The tubes can be represented as upright rigid cylinders. It is assumed that the worms do not extend their fringe, and that all tubes have the same length and diameter.
- The horizontal area of the patch is always exactly rectangle.

- Patches are only seeded where the bed shear stress is smaller than the tide-averaged bed shear stress. At these locations the seedlings will not be eroded due to the water motion.
- The patch reaches its maximum density after one year, but only if all factors to determine the density are most optimal. A maximum tube density has been chosen, concerning field values. The maximum density is 300 ind.m^{-2} , following De Jong et al. (2015).
- Callaway (2003) mentioned that on average 5-13 juveniles were attached to single adult tubes in spring. However not all of the attached juveniles were actual detached to live solitary. The maximum growth rate is 10 juveniles per adult, that means that the recruitment factor should be $R \leq 10$.

4.3 Implementation of *Lanice conchilega* patches

This section describes the method of implementing *Lanice conchilega* into the sand wave model. The location of the patches is dependent on the random seeding in spring. The size of the patch is always at least one grid cell and the amount of bottom covering is approximately 5% of the area. The tube length has fixed value ($L_{tube} = 3.5 \text{ cm}$). The density of the patch has an initial value and it is updated every season. *Lanice conchilega* has three recruitment periods in, spring, summer, and autumn (Van Hoey, 2006). A part of the patch will disappear due to low water temperatures (Strasser and Pieloth, 2001).

Following the method of Borsje (2012) a MORFAC of 182 is used, with this factor one tidal period (12 hours) corresponds to one season (0.25 year). The method is based on two main assumptions. Once a year in spring the percentage of covered bottom is updated. And every season the density of the patch is adapted. The following steps describes the method.

1. First, the model is run during winter without any patches.
2. After winter the tide-averaged bed shear stress is calculated and the worms are seeded where the tide-averaged bed shear stress is smaller than the mean tide-averaged bed shear stress. The calculation of the initial cover in spring is shown in equation 4.8.

$$D_{tube, spring} = D_{tube, initial} \left(\text{chance} = 5\% \quad \text{if} \quad \langle \tau \rangle \leq \text{mean} \langle \tau \rangle \right) \quad (4.8)$$

where:

$D_{tube, initial}$	$[\text{ind.m}^{-2}]$	initial tube density
$\langle \tau \rangle$	$[N \text{ m}^{-2}]$	tide-averaged bed shear stress
$\text{max} \langle \tau \rangle$	$[N \text{ m}^{-2}]$	mean tide-averaged bed shear stress

3. In summer the density of the patch is dependent on the availability of food and the recruitment factor. A measure for the available food is the depth and tide-averaged suspended sediment concentration. Furthermore, a recruitment factor will be used to determine the recruitment of the worms (see equation 4.9).

$$R(D_{tube,spring}) = \frac{D_{max}}{D_{tube,spring} + e^{-D_{max} * a_g * t} * (D_{max} - D_{tube,spring})} \quad (4.9)$$

where:

R	[-]	recruitment factor
α_g	[m ² ind. ⁻¹ days ⁻¹]	growth rate
$D_{tube,spring}$	[ind.m ⁻²]	tube density in spring
D_{max}	[ind.m ⁻²]	maximum tube density

The method of Borsje (2012) assumed that the recruitment factor was always 4, however in this method a growth-curve is used. The calculation of the recruitment factor is shown in section 4.1.1.

Finally, equation 4.10 shows the equation for the adjustment in density in summer. The factor S follows from section 4.1.1 in chapter 6 is stated which one of the two sediment factors is used.

$$D_{tube,summer} = D_{tube,spring} * R(D_{tube,spring}) * S(\langle c \rangle) \quad (4.10)$$

4. In autumn the same procedure is followed as for summer. Again the density is dependent on the recruitment factor and the sediment factor. Equation 4.11 and 4.12 are used.

$$R(D_{tube,summer}) = \frac{D_{max}}{D_{tube,summer} + e^{-D_{max} * a_g * t} * (D_{max} - D_{tube,summer})} \quad (4.11)$$

$$D_{tube,autumn} = D_{tube,summer} * R(D_{tube,summer}) * S(\langle c \rangle) \quad (4.12)$$

5. The method of Borsje (2012) assumed that all tubes disappeared during winter. However other research suggested that patches of *Lanice conchilega* can be classified as reefs (Rabaut et al., 2009; Callaway et al., 2010). This indicates that not all tubes will disappear during winter. In this step, three options are used. The first option (o1, fig. 4.3) is that the patches never disappear, however the tube densities will be lowered with 40%. The second option (o2, fig. 4.3) is that all patches disappear every year. The third method (o3, not explicitly shown in figure) is that every five years all patches disappear, all other years the tube densities are lowered with 40%. The model is one time for every option. Equation 4.13 is used in option one and in option three for four of every five years.

$$D_{tube,winter} = 60\% * D_{tube,autumn} \quad (4.13)$$

6. The next spring, (dependent on option, option 1 goes to step 2) the densities of the patches are updated and new patches are seeded. Firstly, the densities are updated following the same procedure as in summer (eq. 4.14 and 4.15).

$$R(D_{tube,winter}) = \frac{D_{max}}{D_{tube,winter} + e^{-D_{max} * a_g * t} * (D_{max} - D_{tube,winter})} \quad (4.14)$$

$$D_{tube,spring} = D_{tube,winter} * R(D_{tube,winter}) * S(\langle c \rangle) \quad (4.15)$$

Secondly, new patches are randomly seeded at locations where no patches are present yet (eq. 4.16 and 4.17). The same procedure is followed as in the first spring, however the chance of a cell to have a patch is different. It is dependent on the bottom covering growth as explained in section 4.1.2.

$$B(C_{previousyear}) = \frac{C_{max}}{C_{previousyear} + e^{-C_{max}\beta_g t}(C_{max} - C_{previousyear})} \quad (4.16)$$

$$D_{tube,spring} = D_{tube,initial} \left(\text{chance} = B(C_{previousyear}) \quad \text{if } \langle \tau \rangle \leq \text{mean}(\tau) \right) \quad (4.17)$$

where:

B	[-]	seeding factor
β_g	$[\%^{-1} \text{ days}^{-1}]$	growth factor
$C_{previousyear}$	[%]	covering of the bottom in the previous year
C_{max}	[%]	maximum covering of the bottom

7. After spring, the model starts again with step 2.

Figure 4.3 shows a flow chart of the model.

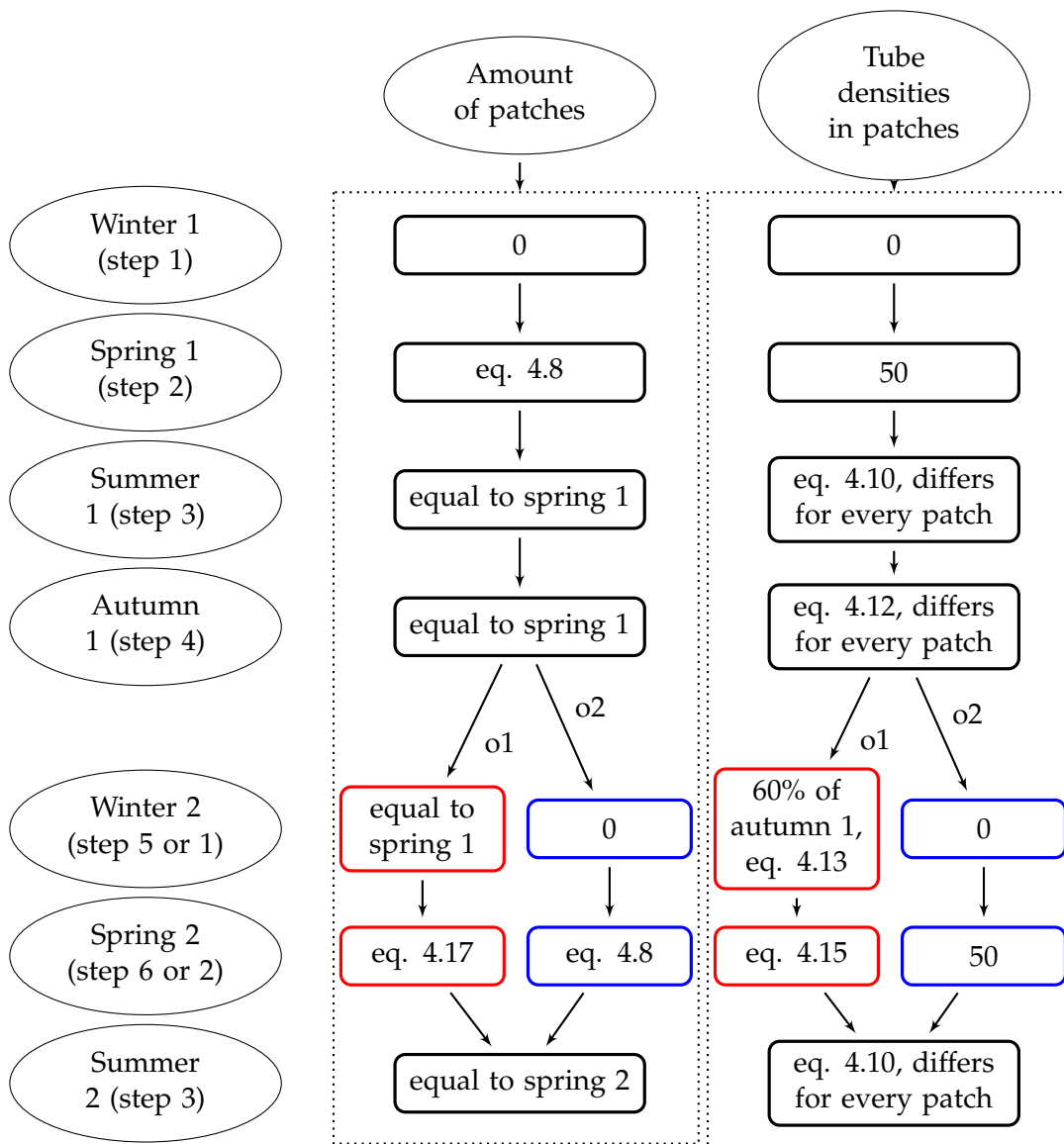


FIGURE 4.3: Flow chart of model equations. The red rectangles contains the equations for option where the patches never disappear. The blue rectangles contains the equations for the option where the patches disappear every year. The third option where all patches disappear every five year is a combination of option one and two, every fifth year option two is used.

CHAPTER 5

Static patches on flat bottoms

This chapter describes the flat bottom case. Section 5.1 shows the bathymetry which is used for this model. Section 5.2 describes the method used. Section 5.3 describes the results of the model runs and finally section 5.4 gives a conclusion.

5.1 Bathymetry

In this chapter we are only interested in the effects of *Lanice conchilega* on the hydrodynamics and the sediment transport, which is stated as the one-way coupling. Therefore, the bathymetry of this model consists of a flat bottom. Figure 5.1 shows the bathymetry with the location of the patch.

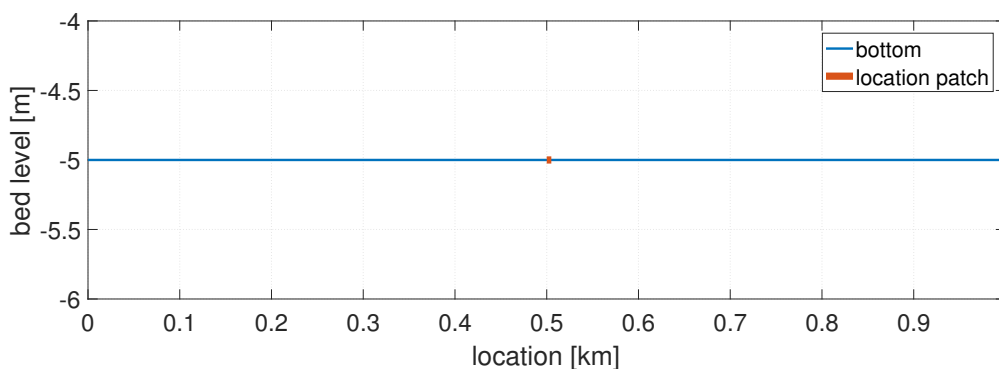


FIGURE 5.1: Bathymetry flat bottom included the location of the patch

5.2 Method

To determine the effects of *Lanice conchilega* on a flat bottom, the Delft3D model, as explained in chapter 3, has been used. The flat bottom set-up has been run for four cases, two with and two without a *Lanice conchilega* patch and both cases are run with and without sediments (tab. 5.1). Case I and case III, both without patch are used to compare the results to a flat bottom with patch, case II and IV. The values used for these cases are shown in table 5.2. After investigating the reference cases,

TABLE 5.1: Four cases used for this bathymetry

Case	I	II	III	IV
Patch	no	yes	no	yes
Sediment	no	no	yes	yes

TABLE 5.2: Parameters settings for reference case and for variable cases (2DV domain)

Parameter	Symbol	Reference value	Variable values	Unit
Physical parameters				
Tidal flow amplitude	U_{S2}	0.65	0.65	[m s ⁻¹]
Water depth	H	25	5	[m]
Sediment grain size	d	350	350	[μ m]
Biological parameters				
Tube diameter	d_{tube}	0.5	0.5	[cm]
Tube length	L_{tube}	3.5	0.5 - 6	[cm]
Tube density	D_{tube}	300	50 - 6000	[ind.m ⁻²]
Patch length	L_{patch}	1	1 - 10	[m]

the parameters tube length, tube density and patch length are varied in case II and IV. Also a second patch has been located on the bottom.

As explained in chapter 3 the tubes of *Lanice conchilega* are modeled as thin, solid piles, which are regularly distributed over the patch. The patch is located in the middle of the domain (fig. 5.1). Borsje et al. (2014a) showed that biological factors are more important for the creation and degradation rates than physical factors. Therefore, only biological factors are varied.

5.3 Results

This section describes the results of the model runs. Section 5.3.1 describes the cases I until IV. Section 5.3.2 describes the variations in case II and IV.

5.3.1 Reference case

The results of case I until IV without variations are described in this section. It is divided into two parts. The hydrodynamic section describes the comparison between case I and II. The morphodynamic section describes the comparison between case III and IV.

Hydrodynamics: Case I and II

Above an undisturbed bed a logarithmic velocity profile and a decreasing turbulence profile is shown (fig. 5.2, blue lines). Within the patch, the bed roughness becomes larger, due to the protruding tubes and therefore the near-bed velocity becomes smaller. The turbulence becomes close to the bottom a bit smaller, but it increases until its maximum value at just below the height of the tubes. The turbulence reaches its maximum value just below the tube height, because the roughness is largest there. The velocity profile and the turbulence profile above a patch are deviated from the profiles without patches as shown in figure 5.2.

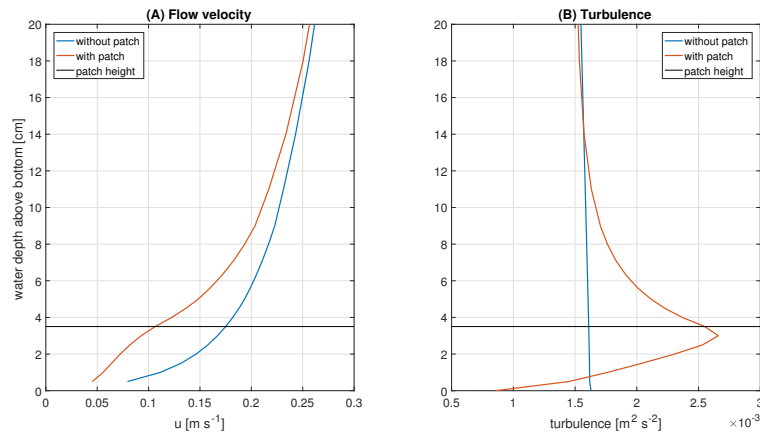


FIGURE 5.2: Flow velocity (A) and turbulence (B) over a flat bottom with and without patch.

The flow velocity along the bottom at a snapshot for maximum flood is shown in figure 5.3. At the leading edge (zero cm in front of the patch, where the water hits the patch first) near the bed, the flow velocity is reduced, whereas higher up into the water column the flow velocity is increased. The decreasing flow velocities near the bed are compensated by the increasing flow velocities higher in the water column. This can be explained by the continuity of the water flow. Within and above the patch the flow velocity is reduced, and this is also compensated by an increased flow velocity above the patch.

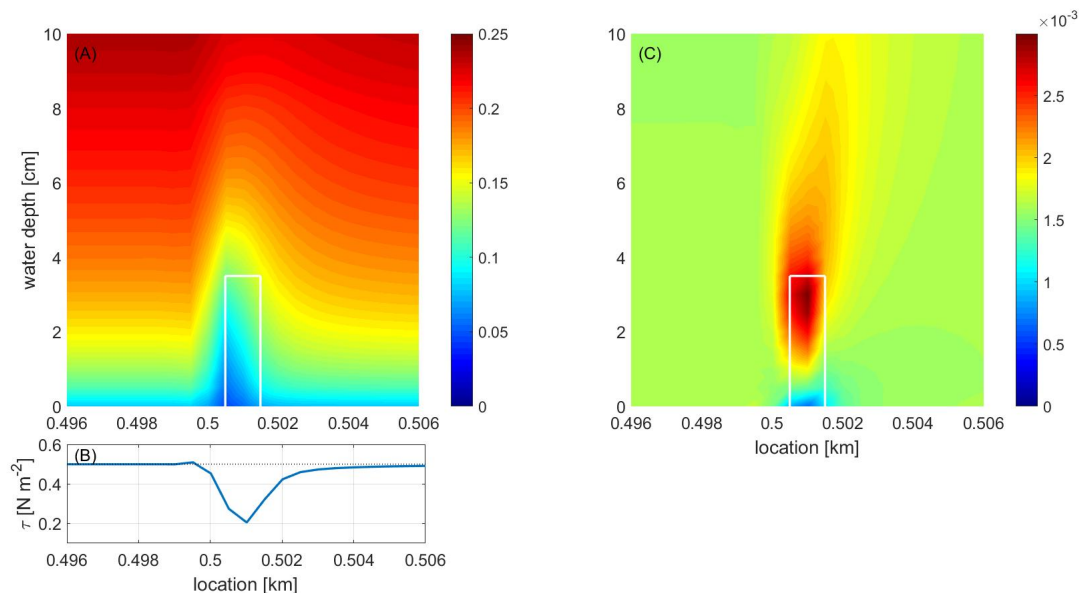


FIGURE 5.3: (A) Horizontal velocity for the maximum flood over a flat bottom with a *Lanice conchilega* patch. For clarity only the lowest 10 centimeter of vertical domain and ten meter in the horizontal domain is shown. The white box represents the *Lanice conchilega* patch. (B) Bed shear stress at the same moment in time. (C) Snapshot of the turbulent kinetic energy.

The bed shear stress (fig. 5.3B) shows a small increase (almost not visible) and a decrease. This can be interpreted as a stabilizing and destabilizing effect. In front of the patch an increase in bed shear stress can be seen because of the accelerated flow velocity. Within the patch a decrease in bed shear stress is shown because within the patch the flow velocity is reduced. In the wake zone (behind the patch, where the water has already flowed through the patch) the bed shear stress is also reduced over a long distance.

Figure 5.4 shows the tide-averaged flow velocity and bed shear stress. During the tidal period the leading edge switches from one side to the other. Therefore the decrease in flow velocity at the leading edge during the first half of the tidal cycle is compensated by the increase in flow velocity in the wake zone during the second half of the tidal cycle.

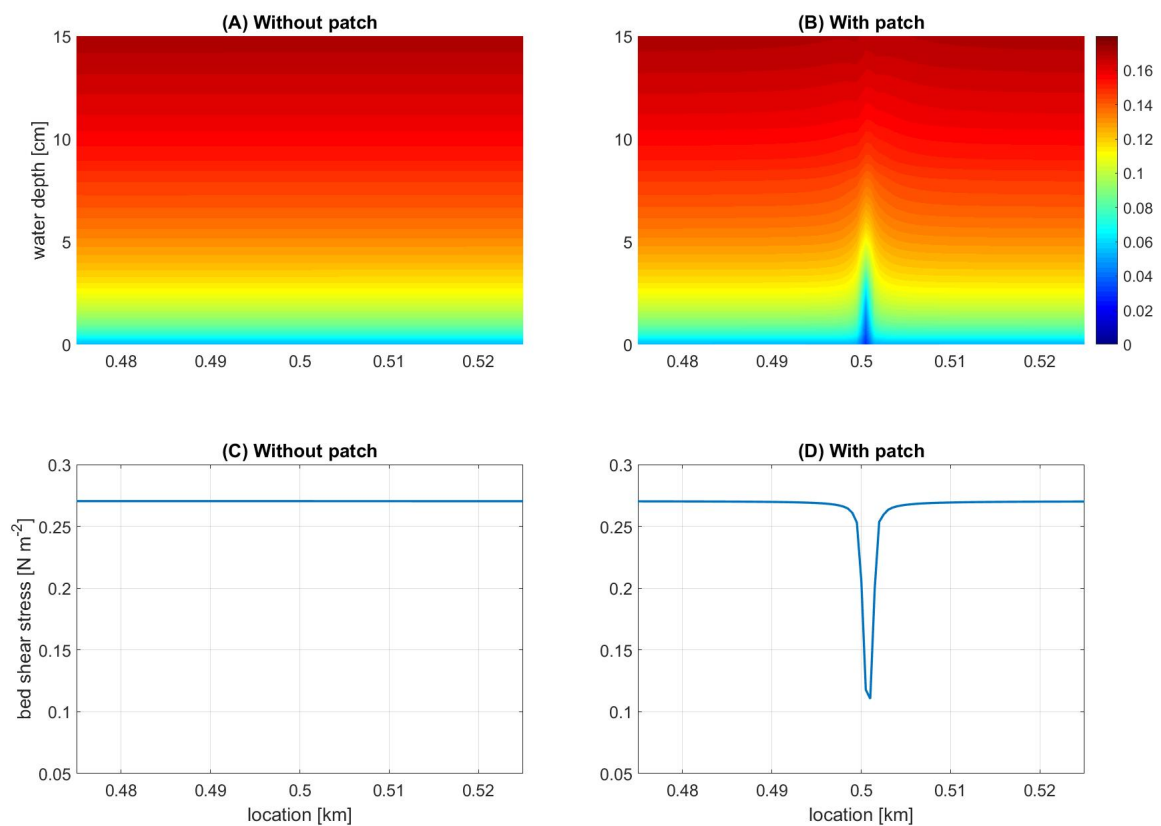


FIGURE 5.4: (A) Tide-averaged horizontal velocity over a flat bottom without patch (case I). (B) Tide-averaged horizontal velocity over a flat bottom with patch (case II). (C) Tide-averaged bed shear stress over a flat bottom without patch (case I). (D) Bed shear stress over a flat bottom with patch (case II). For clarity only the lowest two meters of the water column are shown.

Morphodynamics: Case III and IV

The transport of sediment is largely dependent on the hydrodynamic conditions of the water flow. The tubes of *Lanice conchilega* have large effects on the hydrodynamics, and therefore they also change the sediment dynamics. The bed shear stress and turbulence are important parameters to determine the sediment transport.

The tide-averaged bed load transport within the patch decreases with almost half of its original value (fig. 5.5A). The decrease in bed load transport can be expected from the smaller near-bed velocity and the smaller bed shear stress within the patch. At 20 meters distance of both sides of the patch the bed load transport is still reduced. In the wake zone of the patch the bed shear stress is still decreased for several meters. Because of tidal symmetry, at both sides of the patch the bed load transport is reduced.

The suspended sediment is brought into suspension due to turbulence. As shown in figure 5.2B, the turbulence is largest just below the height of the tubes. Therefore, the suspended load transport shows a peak within the patch (fig. 5.5B). The increased suspended load transport holds for two meters distance of both sides of the patch. So in total there is an increased suspended load transport of five meters along the bottom. After the increase in suspended load transport there is also a decrease at both sides of the patch. The reason therefor is the decreased turbulence.

Furthermore, the suspended sediment concentration is important. Along the bottom with patch (fig. 5.6B), the sediment concentration becomes smaller than along the bottom without patch (fig. 5.6A). The suspended sediment transport rate is larger above the patch, that means that more sediment is transported, and the concentration is less. A patch of one meter width already has a large influence. The suspended sediment concentration reaches its original value after more than 50 meters of both sides of the patch. Therefore, one patch of one meter width has an influence of 100 meters along the bottom.

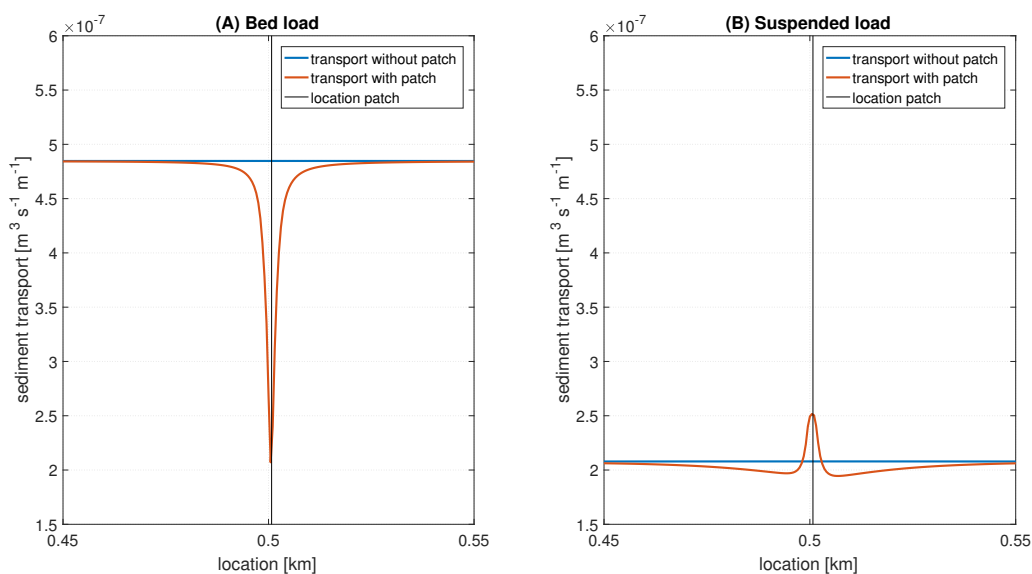


FIGURE 5.5: The tide-averaged sediment transport rates are shown for (A) the bed load transport and (B) the suspended load transport. For parameter settings see table 5.2.

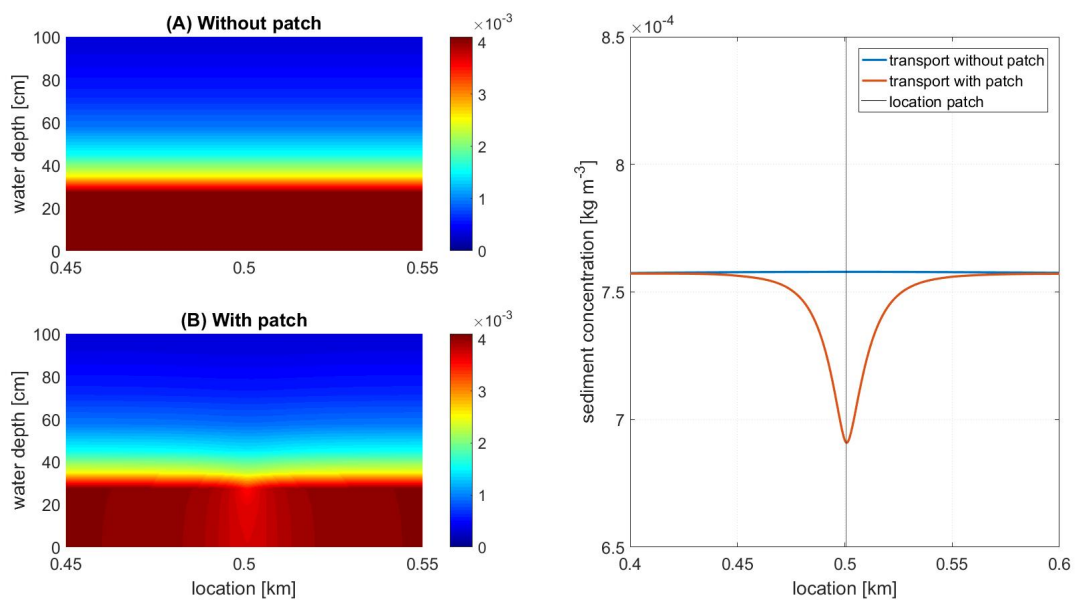


FIGURE 5.6: (A) Tide-averaged suspended sediment concentration without patch, (B) Tide-averaged suspended sediment concentration with patch and (C) Tide- and depth-averaged suspended sediment concentration with and without patch. For parameter settings see table 5.2.

5.3.2 Variable cases

This section describes the results of the variations in case II and case IV. Most of the variations are only done for the hydrodynamic case (case II), because the hydrodynamic parameters are good indicators for the sediment dynamics and this reduces the computational time. For case II, the tube length, density and patch length has been varied. The indicator to describe the differences in varying tube length, density and patch length is the bed shear stress. The bed shear stress is shown in two ways, the absolute values are shown as well as the relative values which are explained as a footprint. The absolute values are shown as the average bed shear stress within a patch (fig. 5.4D).

Footprint

The footprint is defined as the area at both sides of the patch for which the bed shear stress is influenced by more than 1% compared to the bed shear stress without patches, divided by the length of the patch.

Furthermore, a second patch has been added to the bottom where the distance between these two patches has been varied. The indicator to describe the difference for this case is only the absolute bed shear stress. For case IV two contrasting tube densities and tube lengths are chosen to compare the mound heights. The indicator to describe the differences here is the equilibrium mound height.

Case II: Variable tube density

Figure 5.7 shows the decrease in bed shear stress for increasing tube densities. For increasing densities the bottom roughness within the patch becomes larger and therefore the near-bed velocity becomes smaller. Subsequently the bed shear stress becomes smaller as well. Sediment is not taken into account in this case, however larger amounts of sediment will be deposited where smaller near-bed velocities and bed shear stresses occur. Therefore mound heights will grow higher for larger tube densities.

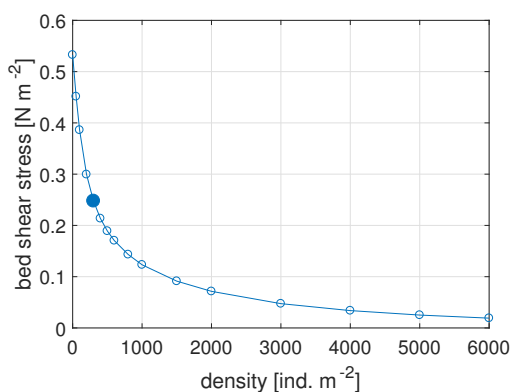


FIGURE 5.7: Variable tube density against bed shear stress. The filled blue dot is the reference case.

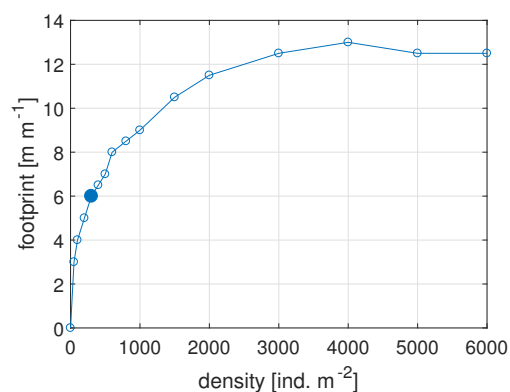


FIGURE 5.8: Variable tube density against footprint. The filled blue dot is the reference case.

For small densities the bed shear stress decreases fast, however for larger densities the bed shear stress decreases less rapidly. Therefore, a nonlinear relationship is suggested between the tube density and the bed shear stress. Only a small amount of individuals per squared meter already has a significant effect on the bed shear stress. A lot more tubes per squared meter does not give such large effects as the first tubes. The reason therefor is that a part of the extra tubes are hidden behind the already present tubes. An extra tube behind another tube does not give the same effect as only one tube in a free stream. This can be stated as the hiding effect.

The footprint of the patch is shown in figure 5.8. The footprint reaches an equilibrium after approximately 3000 ind.m^{-2} . As shown in figure 5.8, the bed shear stress becomes lower for increasing densities, however the opposite effect is shown for the footprint. For increasing densities the footprint is increasing as well. Also this relationship is proposed to be nonlinear. The explanation for this opposite effect is that for larger roughnesses, there is more space needed to regain the original value of the bed shear stress.

Case II: Variable tube length

Figure 5.9 shows the decrease in bed shear stress for increasing tube lengths. The bed shear stress does not decrease as fast as for the tube densities. The reason therefore is that the near-bed flow velocities and near-bed turbulences are approximately the same for each case. The maximum values are the same as well, however for each case it differs at what height in the water column the maximum value occurs, because it occurs at the height of tubes. Furthermore, the variation in tube lengths is much smaller than the variation in tube densities. However, the relationship between the tube length and bed shear stress is still nonlinear.

The footprint for the varying tube lengths is shown in figure 5.10. For increasing tube length the footprint increases as well. This means that larger tubes has a larger range of influence along the bottom. The reason therefor, is that the bed shear stress becomes smaller for increasing tube lengths, so there is more influence along the bottom.

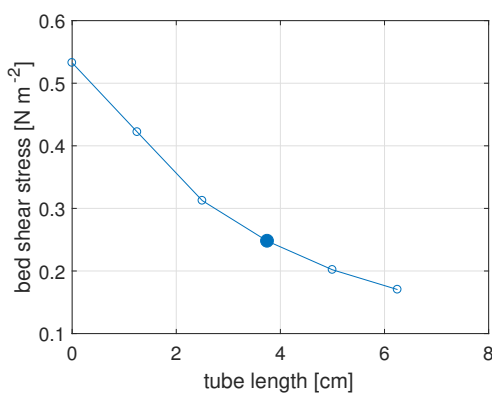


FIGURE 5.9: Variable tube length against bed shear stress.

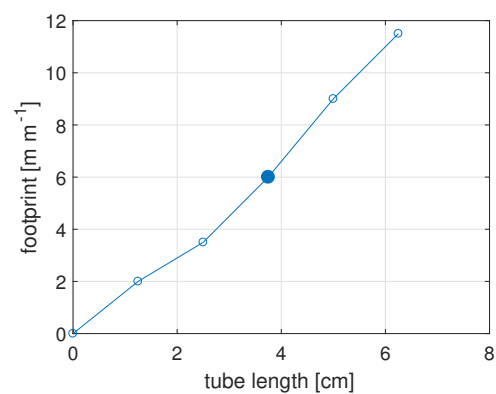


FIGURE 5.10: Variable tube length against footprint.

Case II: Variable patch length

Figure 5.11 shows a decreasing bed shear stress for decreasing patch length. A non-linear relationship is suggested. After a patch length of approximately four meters the bed shear stress does not decrease anymore. From a patch length of four meters or longer, the bed shear stress observed within the patch is not dependent on the length of the patch.

Figure 5.12 shows the footprint of the variable patch lengths. A remarkable result is that the footprint first increases, and thereafter decreases. The absolute value of the bed shear stress increases for increasing patch length. However the relative value of the bed shear stress (is footprint, divided by the patch length) decreases as shown in figure 5.12. Every extra meter of patch length does not have such a large effect anymore on the bed shear stress as the first meter.

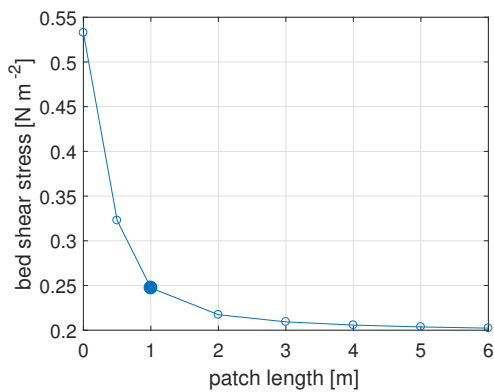


FIGURE 5.11: Variable patch length against bed shear stress. Blue filled dot represents the reference case.

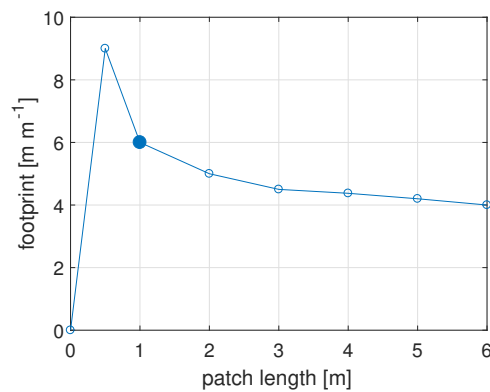


FIGURE 5.12: Variable patch length against footprint. Blue filled dot represents the reference case.

Case II: Multiple patches

Figure 5.13 shows six plots of the tide-averaged bed shear stress with different distances between the two patches. With a distance of one meter between two patches, the bed shear stress does not reach its original shape and values in between the patches. A distance of six meter between the patches shows two graphs of two separate patches. Figure 5.14 shows the average bed shear stress reached between two patches. The footprint of a one meter patch is approximately six. This figure shows that with six meter in between, the original bed shear stress value is reached.

A lower bed shear stress than average means that more sediment will deposit. Between patches, where the bed shear stress does not reach its original value, it is possible that this space will be filled with sediment as well.

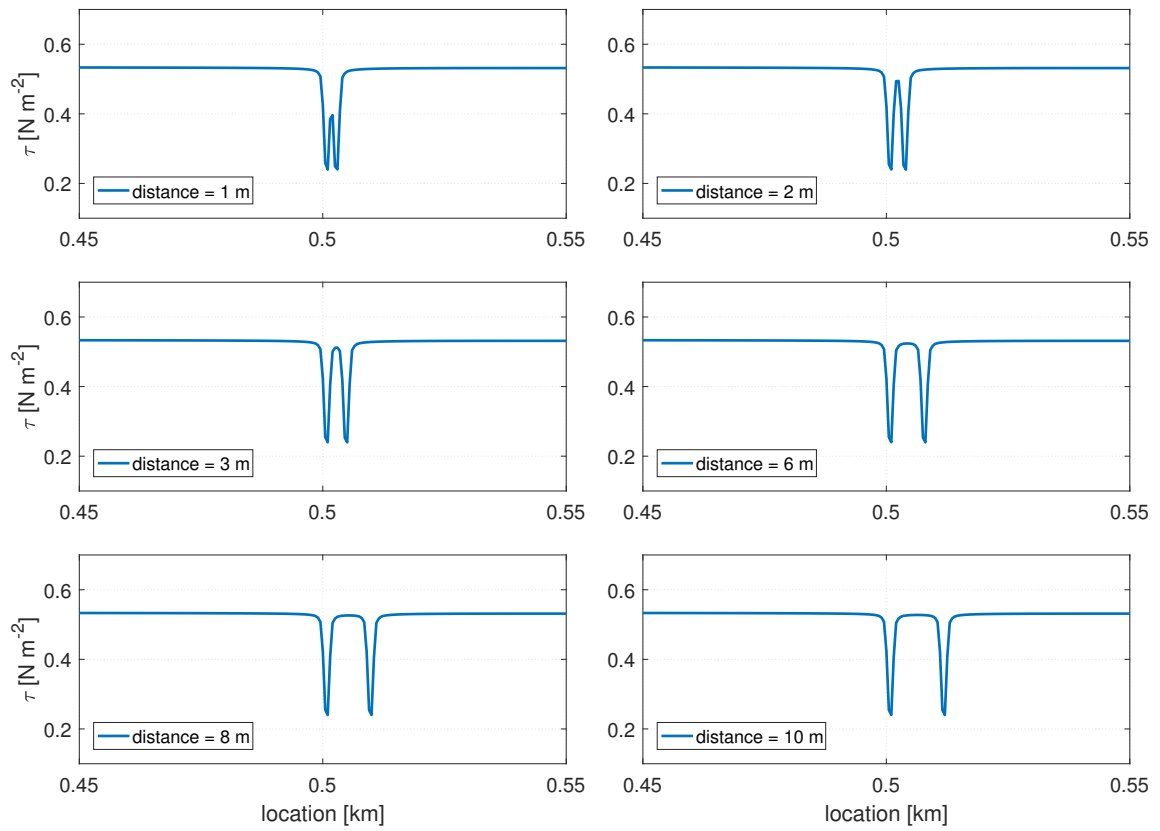


FIGURE 5.13: Tide averaged-bed shear stress for variable distance in between two patches.

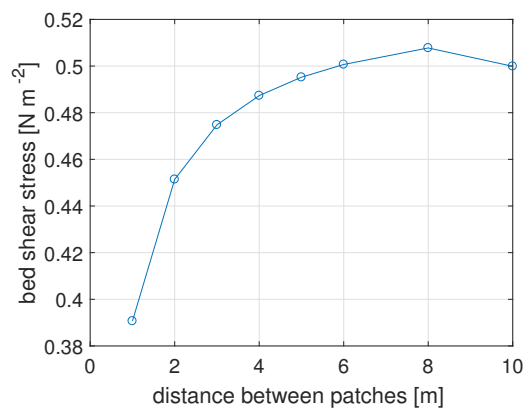


FIGURE 5.14: Average bed shear stress between two patches against distance between two patches.

Case IV: Mound height for varying tube densities and lengths

The mound height has been modeled for two contrasting tube densities (300 and 800 $ind.m^{-2}$) and tube lengths (2.25 and 3.75 cm). In the first weeks, large amounts of sediments were deposited between the tubes. This decreased after a few weeks. The flow velocities over and through the patch were increasing during the growth of the mound. Because of continuity of water flow the growth of the mound is attenuated. As shown in figure 5.15 there is not a real equilibrium reached, and the mounds for a tube length of 3.75 cm and densities of 300 and 800 $ind.m^{-2}$ are over predicted compared to field values. This has one main reason. The tubes always protrude the modeled length from the sediment and the water depth is relatively large. It means that there is no restricting value for the mound to stop growing. Furthermore, the water flow only goes over and through the patch. In reality the water flow goes also around the patch. The equilibrium mound height with a tube length of 2.5 cm shows agreement with field studies.

Figure 5.16 shows the mounds for the contrasting tube densities and lengths. A remarkable result is that at the bottom of the mound, it is much wider than the original width of the patch. The reason therefor is that in front of the patch, the velocity slow down, through which the sediment deposits. Furthermore, erosion holes are formed at both sides of the mound, this is in agreement with field studies.

A tube density of 800 $ind.m^{-2}$ gives a larger mound height than a tube density of 300 $ind.m^{-2}$. This also follows from the smaller bed shear stress for a larger density, found in previously. The same effect is found for different tube lengths. Larger tube lengths give a larger mound height.

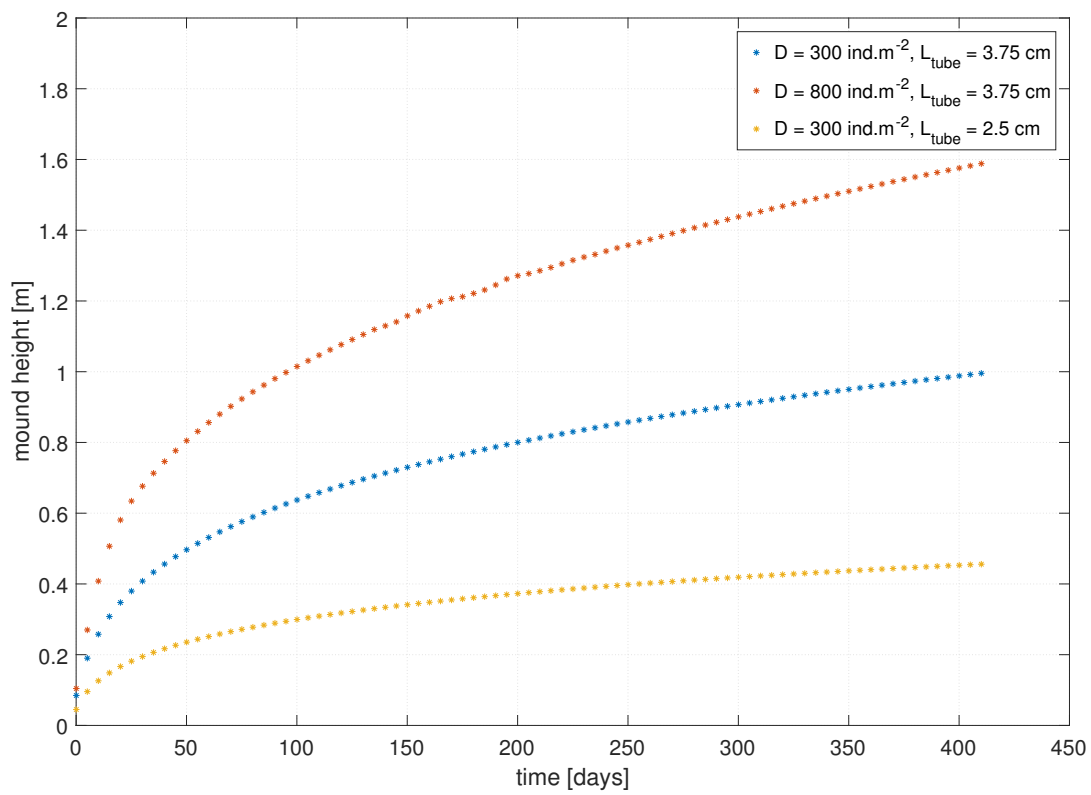


FIGURE 5.15: Equilibrium mound height for varying tube densities and tube lengths.

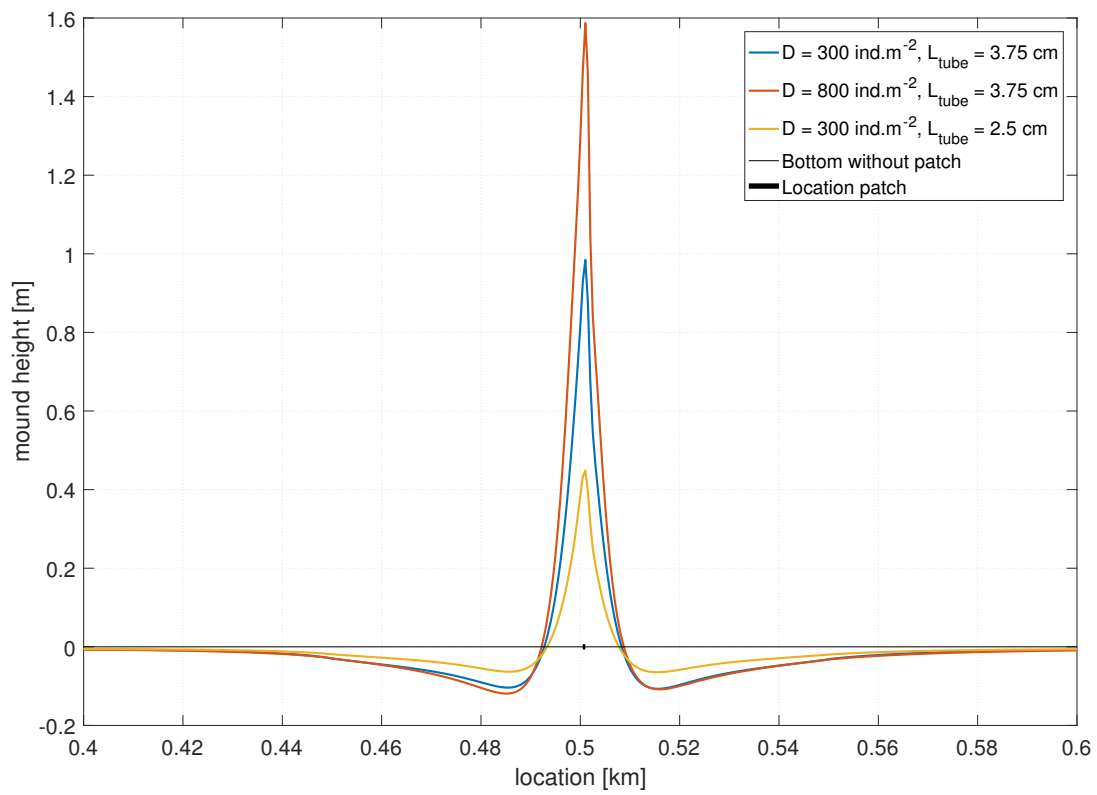


FIGURE 5.16: Mound height for varying tube densities and tube lengths.

5.4 Conclusion

The tubes of the *Lanice conchilega* worm within a patch are able to change the hydrodynamics and therewith the sediment dynamics. The protruding tubes from the sediment cause more bottom roughness, therefore the velocity is decreased within the patch and the turbulence is increasing to maximum value at the height of the tubes.

From the model can be concluded that the tubes have significant effects on the hydrodynamics. Within the patch, the flow velocity and the bed shear stress is decreased, and this keeps on for several meters along the bottom. The turbulence is increasing to its maximum value at the height of the tubes. Higher up into the water column the turbulence is decreasing again. These changes in water velocity, bed shear stress and turbulence cause alterations in the sediment transport. The bed load transport is largely decreased within a patch, due to the lower near-bed velocities. The suspended load transport is increased above the patch, due to more turbulence. At both sides of the patch, the suspended load is decreased, because of lower turbulence.

The hydrodynamics determine for a large part the sediment transport. Therefore, the variations in tube length, tube densities, patch length, and distance between two patches is only done for the hydrodynamic case in order to reduce the computational time. Tube densities were important for the decrease in bed shear stress, as long as the densities were small. For larger tube densities the bed shear stress reaches an equilibrium. This suggests that the relationship between the tube densities and bed shear stress is nonlinear. Tube length was always important, the decrease in bed shear stress was almost linear. For larger tube lengths the decrease is attenuated, however these do not occur in the field. The relationship between the bed shear stress and the patch length, is suggested to be nonlinear. The minimum bed shear stress within a patch has a minimum value, independent on the length of the patch. However, patches of two meters or longer are not found in the field, the average patch size measured in the field was $1.37 m^2$ (Rabaut, 2009). The bed shear stress between two patches reaches its original value if the distance is three meter or more. If patches have less than 3 meter in between, the space can be filled up with sediment.

The second indicator to compare the varying cases was the footprint. The footprint shows how many meters along the bottom per meter patch width the bed shear stress is influenced. The largest footprint values were reached by the tube densities compared to the tube lengths and patch length. However, only densities of up to $1000 ind.m^{-2}$ are frequently measured in the field (De Jong et al., 2015).

Mounds are formed due to the sediment which is deposited between the tubes in a patch. Larger tube densities and lengths give larger mound heights. The erosion holes were in agreement with field studies. The mounds with a larger tube length (3.75 cm) were over predicted compared to field data. The mound with a smaller tube density (2.5 cm) was equal to field data.

CHAPTER 6

Dynamic patches in sand waves

This chapter describes the sinusoidal bottom and self-organizational bottom case. Section 6.1 shows the bathymetries used in this chapter. Section 6.2 explains the methods used. Section 6.3 compares the two different sediment factors. Section 6.4 shows the results of the morphological development and finally section 6.5 contains the conclusions.

6.1 Bathymetry

A sinusoidal and self-organizational bottom are used as initial bathymetries for this chapter. Three different sand wave heights are used: $H_{wave} = 0.5, 2, \text{ and } 5 \text{ m}$ (fig. 6.1). The sand wave length is $L_{wave} = 309 \text{ m}$, which is the fastest growing mode in this system (Van Gerwen et al., 2016). The initial bathymetry of the self-organizational bottom exist of arbitrarily superimposed and sized perturbations taken from a Gaussian distribution, scaled to a maximum amplitude of 2 meters. The range of wave lengths is between 50 and 600 meters (fig. 6.2).

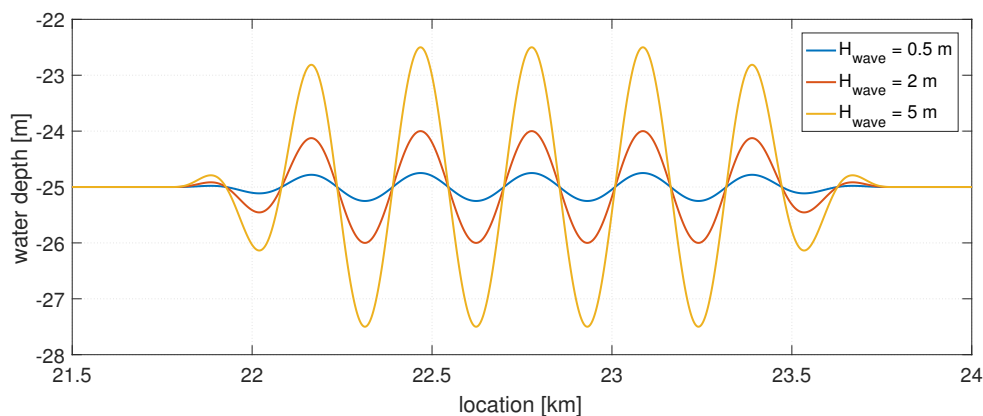


FIGURE 6.1: Initial bathymetry with sand wave height $H = 0.5, 2, 5 \text{ m}$ and wave length $L = 309 \text{ m}$.

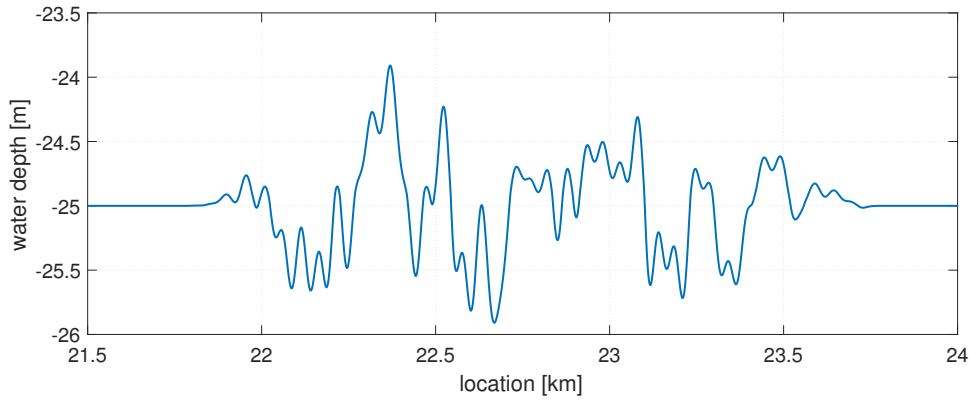


FIGURE 6.2: Initial bathymetry for the self-organizational sand wave with maximum sand wave height of 2 meter and sand wave lengths between 50 and 600 meter.

6.2 Method

Dynamic patches of *Lanice conchilega* are implemented in the sand wave model following the method explained in detail in section 4.3. The parameter settings are shown in table 6.1.

Firstly, all three cases (tab. 6.2) are run for one year of morphological development. All cases are run both with sediment factor one and with sediment factor two (tab. 6.3). So, in total six model runs has been done for one year of morphological development. The three bathymetries are used to investigate the difference of the two sediment factors. Subsequently, the model runs are used to determine which sediment factor is the most realistic one. This part is explained in section 6.3.

Secondly, two bathymetries are run for 20 years of morphological development. The two bathymetries are the sinusoidal bottom with a wave height of two meter (case II, tab. 6.2) and the self-organisational bottom (fig. 6.2). As explained in section 4.3 at step five, three options are used for how often the patches disappear (tab. 6.4). These three options are compared in order to say something about which one is the most realistic. This part is explained in section 6.4.

TABLE 6.1: Parameter settings

Parameter	Symbol	Reference value	Variable values	Unit
Physical parameters				
Tidal flow amplitude	U_{S2}	0.65	0.65	[m s ⁻¹]
Water depth	H	25	25	[m]
Grain size	d	350	350	[μ m]
Wave height	H_{wave}	2	0.5 ; 2 ; 5	[m]
Wave length	L_{wave}	309	309	[m]
Ecological parameters				
Tube diameter	d_{tube}	0.5	0.5	[cm]
Tube length	L_{tube}	3.5	3.5	[cm]
Maximum tube density	D_{max}	300	0 - 300	[ind.m ⁻²]
Patch length	L_{patch}	2	2	[m]

TABLE 6.2: Three cases for sinusoidal bottom

Case	I	II	III
H_{wave} [m]	0.5	2	5
D_{max} [$ind.m^{-2}$]	300	300	300

TABLE 6.3: Sediment factor equations

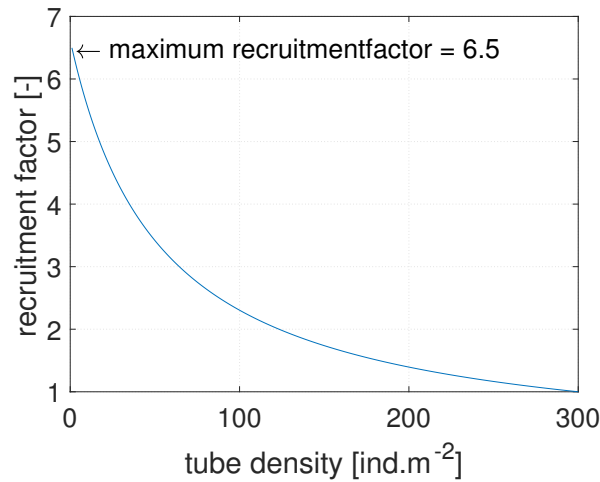
Sediment factor 1 (eq. 4.4)	Sediment factor 2 (eq. 4.5)
$S(\langle c \rangle) = \frac{\langle c \rangle}{\max\langle c \rangle}$	$S(\langle c \rangle) = \frac{\langle c \rangle}{\text{mean}\langle c \rangle}$ for $0,4 < S < 1$

TABLE 6.4: Three options for how often patches disappear, used for 20 years of morphological development.

Option 1	Option 2	Option 3
Patches never disappear	All patches disappear every year	All patches disappear every 5 years

6.3 Results: Comparison sediment factors

The tube density growth factor (recruitment factor multiplied by sediment factor, eq. 4.1) for sediment factor one and sediment factor two (tab. 6.3) has been compared in order to study which one is the most realistic. First, the recruitment factor is shown in figure 6.3. For increasing tube densities the recruitment factor decreases, this follows from the logistic growth curve.

FIGURE 6.3: Decreasing recruitment factor for increasing tube densities until a maximum density of $300ind.m^{-2}$.

Secondly, the sediment factor is required for the growth factor (fig. 6.4B for sediment factor 1 and 6.4C for sediment factor 2). Figure 6.4A shows the tide- and depth-averaged sediment concentration for a bottom without any patches. If patches are located, the sediment concentration becomes different. At locations where mounds arise the sediment concentration becomes larger. Figure 6.4B shows clearly that for sediment factor one and a wave height of two and five meters, the sediment factor

becomes smaller than 0.4 in the troughs. The reason that the sediment factor becomes this low is because of the range of the sediment concentration for the wave heights of two and five meter. In the troughs a small value is divided by a large value (see eq. in tab. 6.3), which give small sediment factors. For the wave height of 0.5 meter, the range is small, so the differences of the sediment factor in the troughs and crests are small. Sediment factor two never becomes lower than 0.4 due to the given restriction (tab. 6.3).

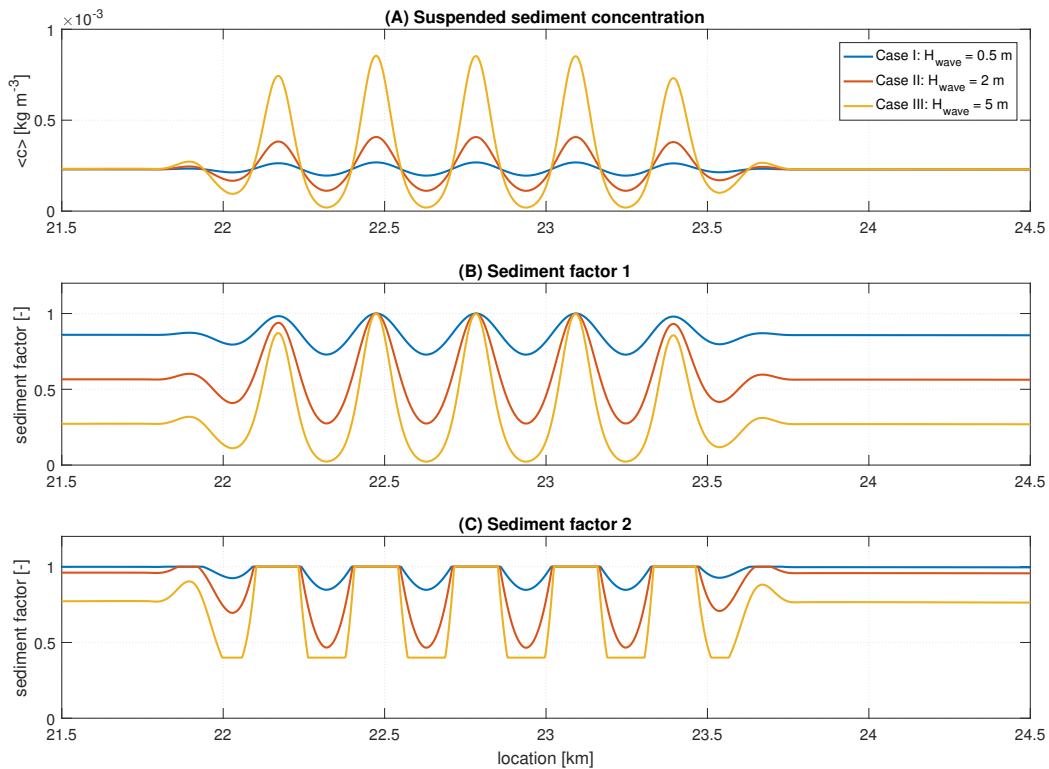


FIGURE 6.4: (A) Tide- and depth-averaged suspended sediment concentration along the bottom without patches of *Lanice conchilega*. (B) Sediment factor one. (C) Sediment factor two.

Finally, the tube density growth factors are shown in figure 6.5. The green diamond is the recruitment factor and the purple circle is the sediment factor. These two multiplied equals the tube density growth factor represented by the light blue square. Figures C and E have both very small sediment factors as explained previously. When densities are small, the recruitment factor becomes large (see fig. 6.3). The large value of the recruitment factor is trying to compensate for the very low sediment factor. Figures D and F are the same cases, respectively as C and E (same wave heights), however in these (D and F) cases the sediment factor does not become lower than 0.4, due to the restrictions. Therefore the recruitment factor does not become as high as in figures C and E. In figures C and E the total growth factor is around or below one, whereas the total growth factors in figures D and F are above zero. As explained previously, this difference is due to the sediment factor. The growth or decay of the patch is dependent on the growth factor larger or smaller than one. The most important point from this figure is the difference in values of the light blue squares between the three figures at the left hand side and the three

figures at the right hand side. The light blue square indicates whether a patch will grow or decay.

This is an example for the tube density growth factor from summer to autumn in the first year. Every season the recruitment factor differs, due to the dependency on the density of the previous season. The sediment factor differs every season because the suspended sediment concentration becomes larger where mounds arise. Therefore the sediment factor becomes larger as well.

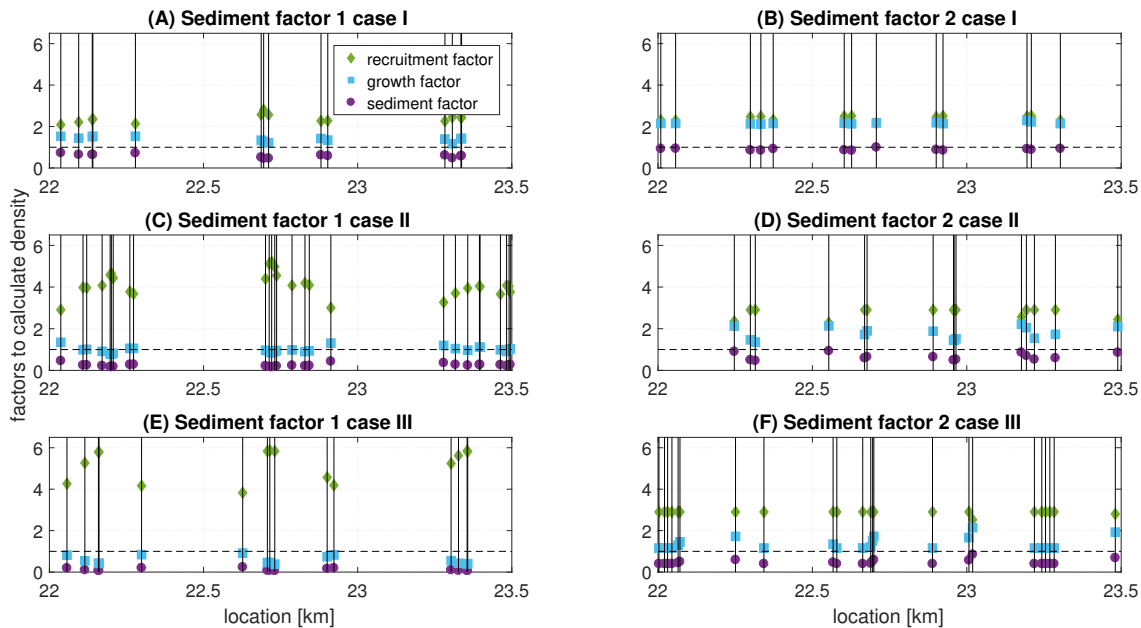


FIGURE 6.5: All growth factors for sediment factor 1 en 2, case I, II and III. The green diamonds represent the recruitment factor, the purple circle the sediment factor, and the light blue square represents the total growth factor, which is the multiplication of the recruitment and sediment factor. The vertical black line are the locations of the patches. If the light blue square is above the horizontal black dotted line, the tube density grows, otherwise it will decay.

The density during the year in all patches is shown in figure 6.6. For both sediment factors and all cases the maximum density is not reached after one year. Another remarkable result is that for sediment factor one and a wave height of two and five meter (case II and III) the patch density becomes lower than the initial density in spring. For case II the density varies between 6 and 79 ind.m^{-2} and for case III the density varies between 2 and 35 ind.m^{-2} . Because the value of sediment factor one becomes very low in the troughs, the tube densities within the patches becomes low. For all other cases the densities stay larger than the initial density.

This model only uses one grain size, therefore the results with sediment factor one (tab. 6.3) are not accurate enough. In reality the troughs of sand waves consist of finer-grained and less well-sorted sediment (Roos et al., 2007). This means that there is more sediment available as food for the worms. Using more grain sizes the effect of less well-sorted troughs can be addressed in the model. However, due to computational time this was not possible.

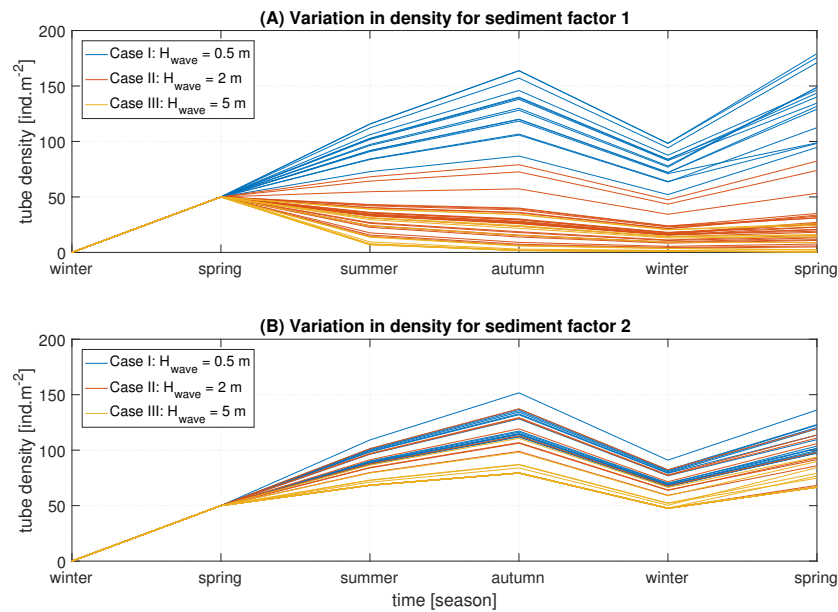


FIGURE 6.6: Every line represents one patch and shows the variation in density during the year. The colors indicate in which case the patches are present.

Determination method used further on

From the comparison of the two sediment factors, it can be concluded that sediment factor two (tab. 6.3) gives the most realistic values. In spring, summer and autumn the patch grows and does not decay. Therefore sediment factor two is chosen to use in the next section.

6.4 Results: Morphological development

Two bathymetries are chosen to run for the morphological development on the long term. The first is a sand wave with a height of two meter and a sand wave length of 300 meter (fig. 6.1). The second is a selforganisational bottom with a maximum wave height of two meter and a variable wave length between 50 and 600 meter (fig. 6.2).

6.4.1 Sinusoidal bottom

The sinusoidal bottom case was run for ten years with a wave height of two meter and a maximum density of 300 ind.m⁻². Three models were run as shown in the method (tab. 6.4). First of all, for all three options, the results after one year of morphological development are analyzed (fig. 6.7). Mounds are already formed after one year of morphological development, the maximum observed mound height was 60 cm. The mound heights half-way the flanks were slightly larger than the mound heights in the troughs. The height of these mounds are comparable with field values (Degraer et al., 2008; Rabaut, 2009). Erosion holes are formed at both sides of the mound, which is also in agreement with field studies (Rabaut et al., 2007). It occurs that patches are next to each other with only one or two grid cells (two meter per

grid cell) in between. This space without tubes is, however, filled with deposited sediment as well. The reason therefor is that the bed shear stress between these two patches stays low as well (sec. 5.3.2; Case II: Multiple patches). Hence, the flat bottom model used a grid cell width of 0.5 meter and this model used a grid cell width of two meter, which means that the flat bottom model is more accurate with the bed shear stress between two patches.

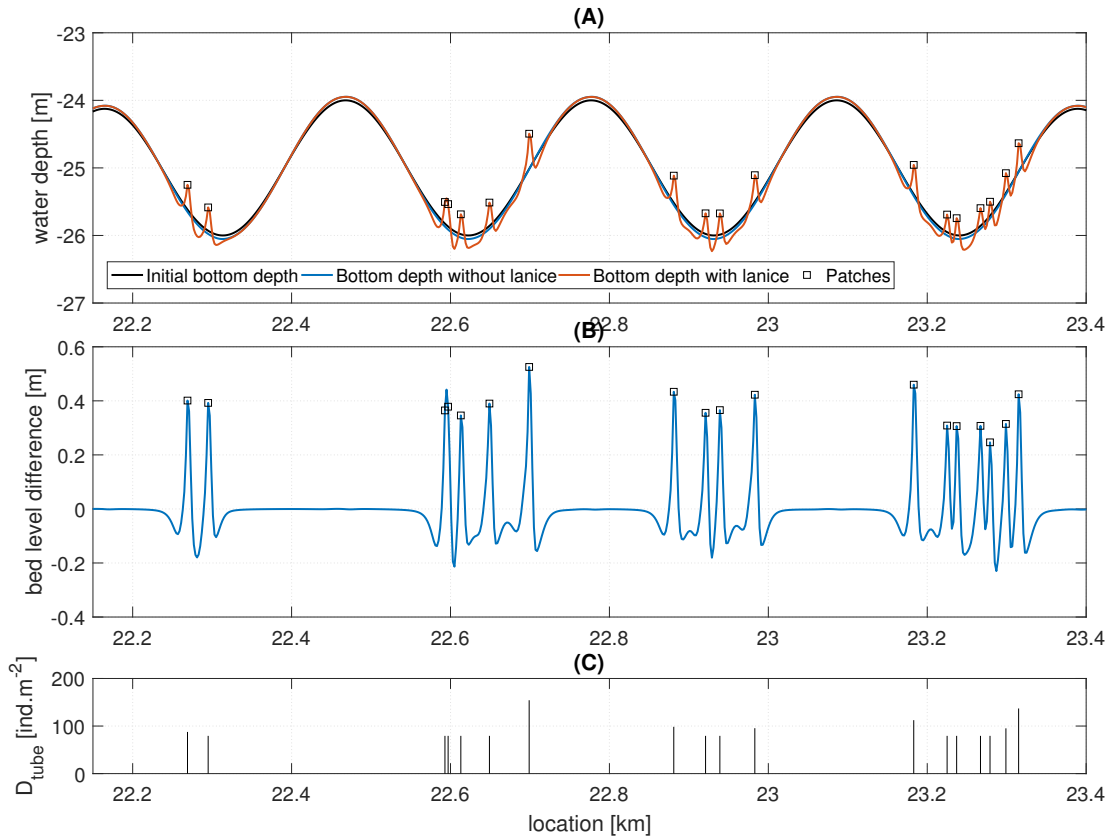


FIGURE 6.7: (A) Bottom depth after one year of morphological development. (B) Difference between morphological development with and without patches. (C) Densities in autumn.

In the troughs the tube densities are up to 80 ind.m^{-2} , and halfway the flanks the tube densities are up to 150 ind.m^{-2} after one year (fig. 6.7C). Tube densities are higher halfway the flank, because more sediment is available as food, through which the tube densities grow faster (sec. 6.3). This also explains why the mound heights are slightly larger on the flanks than on the troughs. Mounds become higher were the densities are larger (sec. 5.3.2). At locations where patches are absent, the bed levels are equal to the sand waves without patches. This indicates that the bed levels are only locally changed after one year of morphological development.

The bottom with one year of morphological development with patches, as shown in figure 6.7, is afterwards run without tubes. Figure 6.8 shows how fast the mounds disappear. Halfway the flanks it takes less than one year for a mound to disappear after all tubes have left the mound. Within the troughs it takes approximately two years for a mound to disappear. The reason for the difference in degradation time is the relatively higher bed shear stress halfway the flanks and the relatively lower bed shear stress within the troughs. Because of the higher bed shear stress halfway

the flanks, the sediment is eroded more easily. This means that the mounds halfway the flank disappear faster than in the troughs.

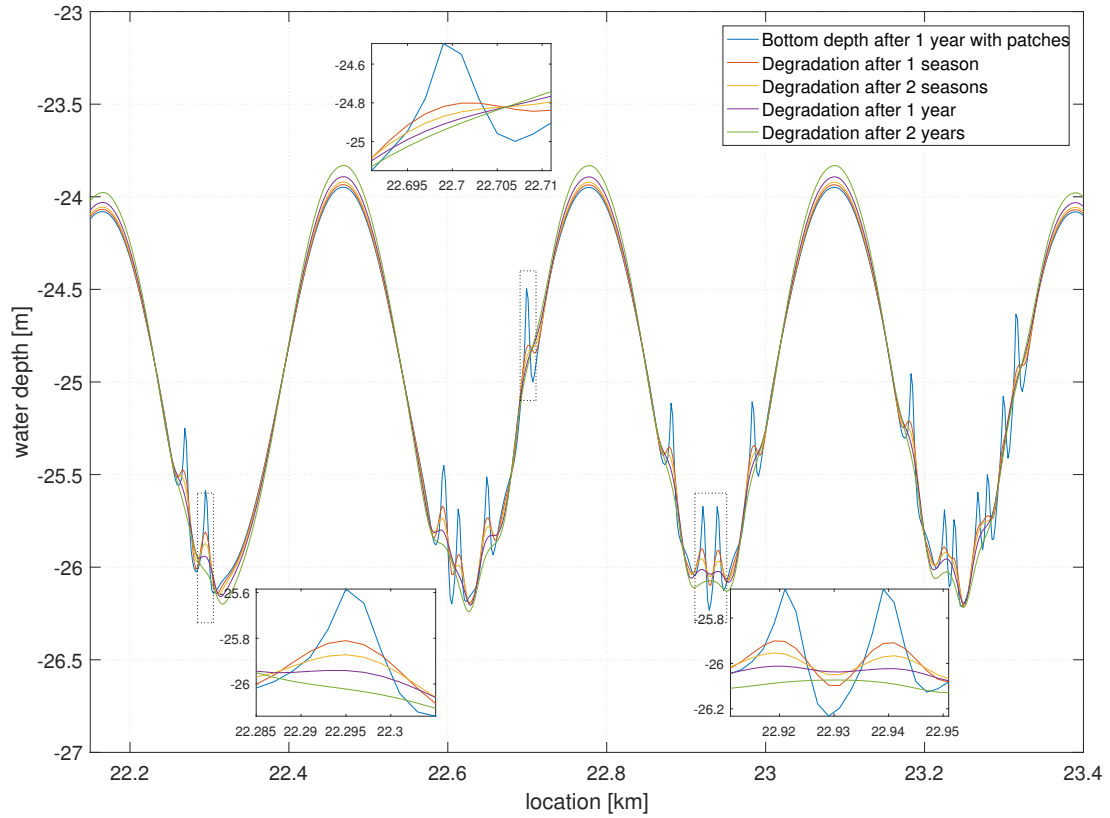


FIGURE 6.8: The tubes are disappeared from all mounds, the degradation in mounds are shown. Three mounds are enlarged to show the difference between mounds halfway the flank and in a trough.

Option one after ten years

The morphological development after ten years is analyzed separately for the three options of how often the patches disappear. For the first option (tab. 6.4), the patches never disappeared (fig. 6.9). After ten years, the mounds were up to seven meters high (fig. 6.9B). These values are over-predicted compared to field values. The reason that the mounds grow this high is that the tubes always protrude the modeled length from the sediment. However, in reality the worms have a maximum length, which means that at some point the worms and therewith the tubes stop growing. As shown in section 5.3.2 (Case IV: Mound height), there was not an exact equilibrium reached, therefore the mounds can grow this high.

Furthermore, in reality the patches will not last for ten years at one spot. Moreover, the tubes are initially located where the bed shear stress is lower than the tide-averaged. After the growth of the mound, the bed shear stress becomes higher at the location of the patch, therefore the location is not preferred anymore by the worms. In reality the worms will disappear or move. However, in this model this effect is not taken into account. The densities in this case were up to 280 ind.m^{-2} (fig. 6.9C).

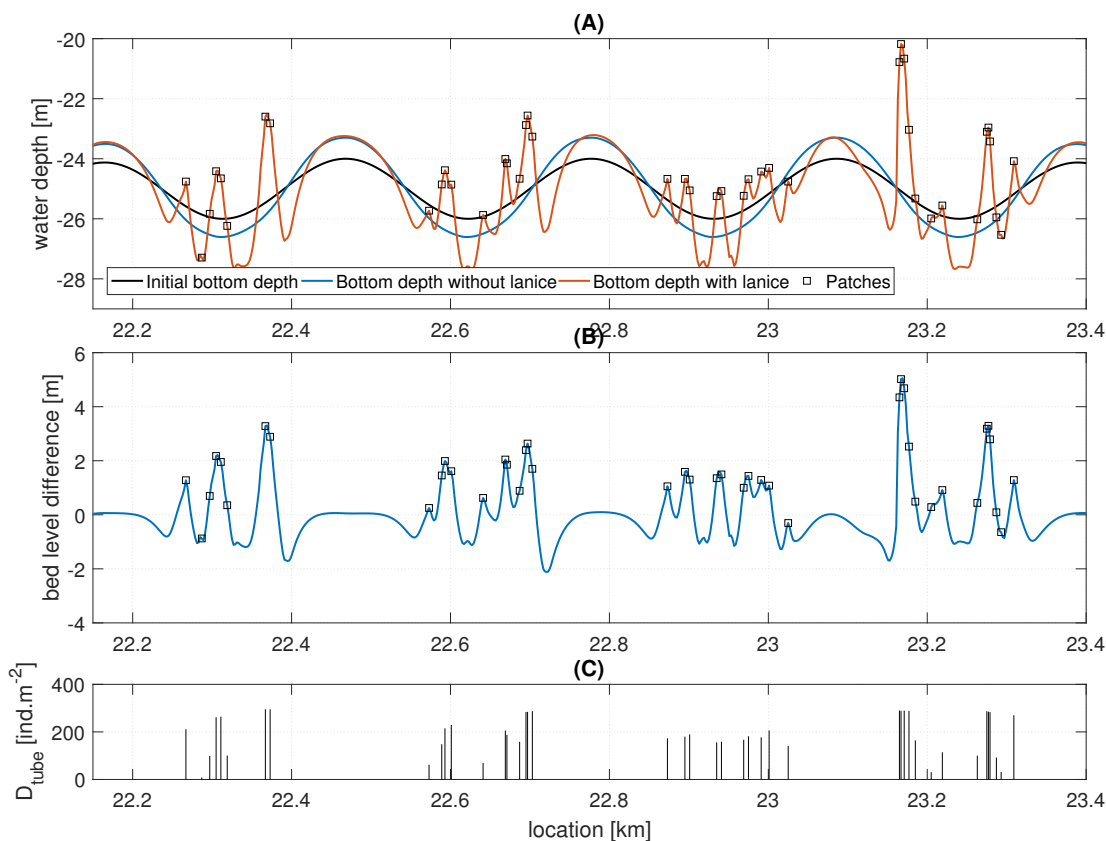


FIGURE 6.9: Morphological development after ten years, where the patches never disappear. (A) Shows the development with *Lanice conchilega* (orange line) and without (blue line). The squares show the locations of the patches. (B) The bed level difference with and without *Lanice conchilega*. (C) The densities in autumn for all ten years.

Option two after ten years

For the second option (tab. 6.4), all patches disappear every year (fig. 6.10). After ten years the maximum mound height is slightly larger, compared to the first year. The maximum mound height after ten years is one meter. The reason that the maximum mound height is slightly larger than after one year, is because new patches are also located on mounds of the previous year. Therefore, the mounds grow higher than after only one year. These mound heights are in accordance with field values (Degraer et al., 2008; Rabaut, 2009). Due to the varying locations of the mounds, the troughs of the sand waves become irregular.

The densities in this case were up to 75 ind.m^{-2} in the troughs, half-way the flanks the densities were somewhat larger up to 130 ind.m^{-2} . The differences in densities are due to the sediment factor which is always smaller in the troughs of the sand waves.

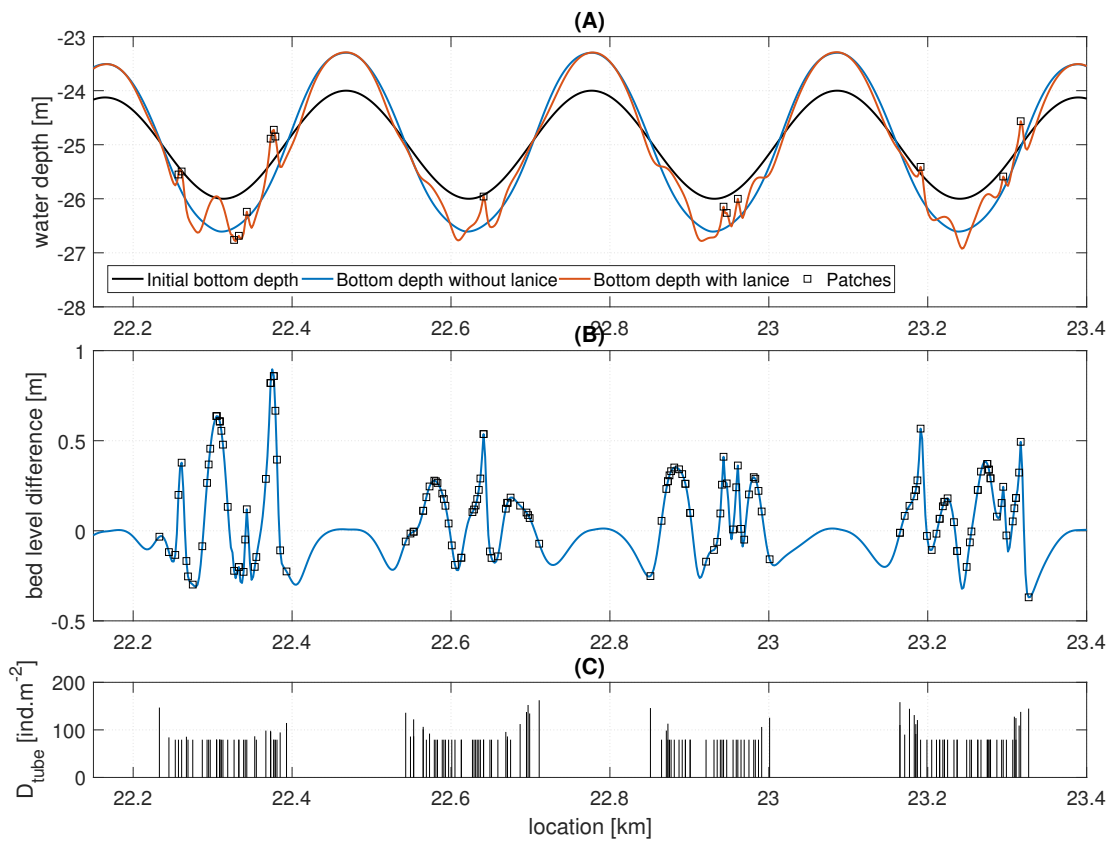


FIGURE 6.10: Morphological development after ten years, where the patches disappear every year. (A) Shows the development with *Lanice conchilega* (orange line) and without (blue line). The squares show the locations of the patches in year ten. (B) The bed level difference with and without *Lanice conchilega*. (C) The densities in autumn for all ten years.

Option three after ten years

For the last option (tab. 6.4), every five years all patches disappear (fig. 6.11). After ten years most of the mounds have a height of 1.5 meter. However, there are two outliers, which have heights of more than three meters. Compared to field values, both of these values are over predicted. The outliers are half-way the flank, where more sediment is available and densities grow faster. However, the bed shear stress at these locations is not preferred by the worms anymore.

The other mounds are a bit over predicted as well. The reason therefore is that the worms does not stop growing, and the tubes protrude always the modeled length from the sediment.

The tube densities were in this model also dependent on the location. The densities in the troughs are up to 80 ind.m^{-2} and half-way the flanks the densities reach the maximum of 300 ind.m^{-2} .

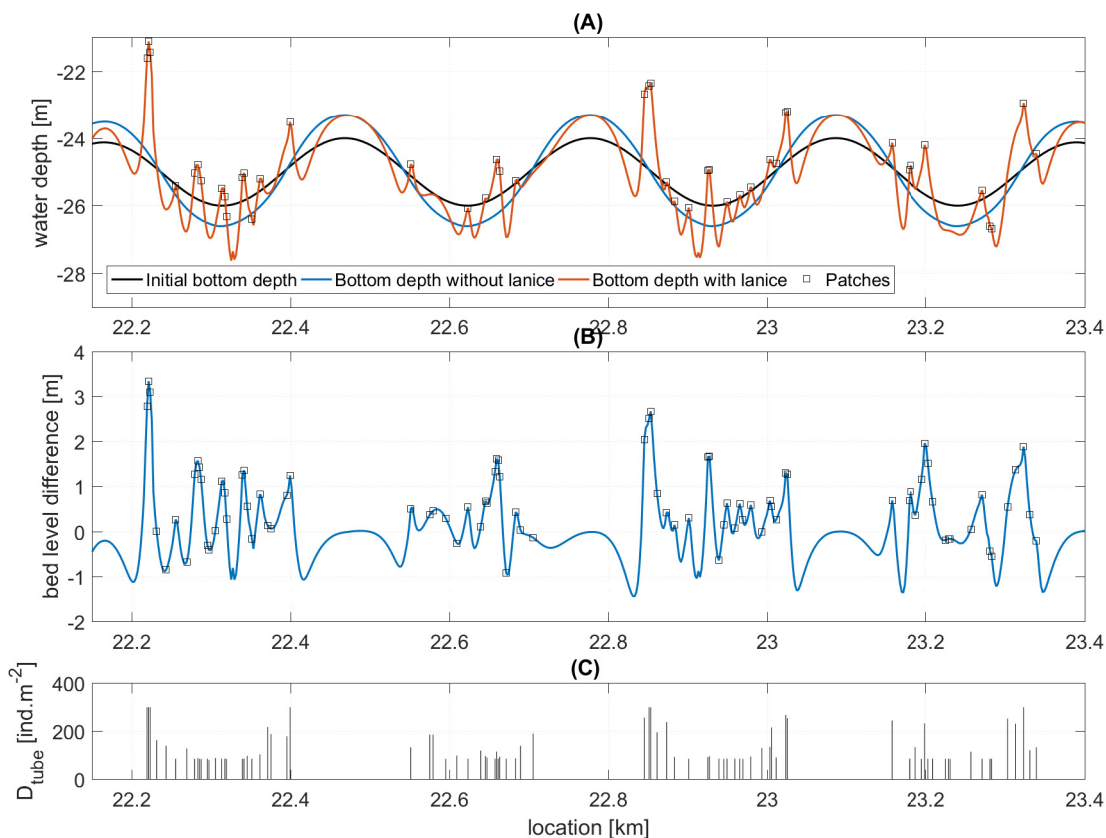


FIGURE 6.11: Morphological development after ten years, where the patches disappear every five years. (A) Shows the development with *Lanice conchilega* (orange line) and without (blue line). The squares show the locations of the patches in year ten. (B) The bed level difference with and without *Lanice conchilega*.

6.4.2 Self-organisational bottom

The self-organisational bottom case was run for 20 years with a maximum wave height of two meter and a variable wave length between 50 and 600 meter. With this bathymetry, two of the three options (tab. 6.4, option two and three) were run. As well as for the sinusoidal bottom, first of all, the results after one year of morphological development are analyzed (fig. 6.12). Also in this model, mounds are already formed after one year of morphological development. The maximum observed mound height is 65 cm, this is comparable with the sinusoidal bottom case and field values (Degraer et al., 2008; Rabaut, 2009). Also erosion holes are formed, which is also comparable with the sinusoidal bottom case and field observations (Rabaut et al., 2007). In this model no patches appeared to be very close to each other, such that the space between them is filled with sediment.

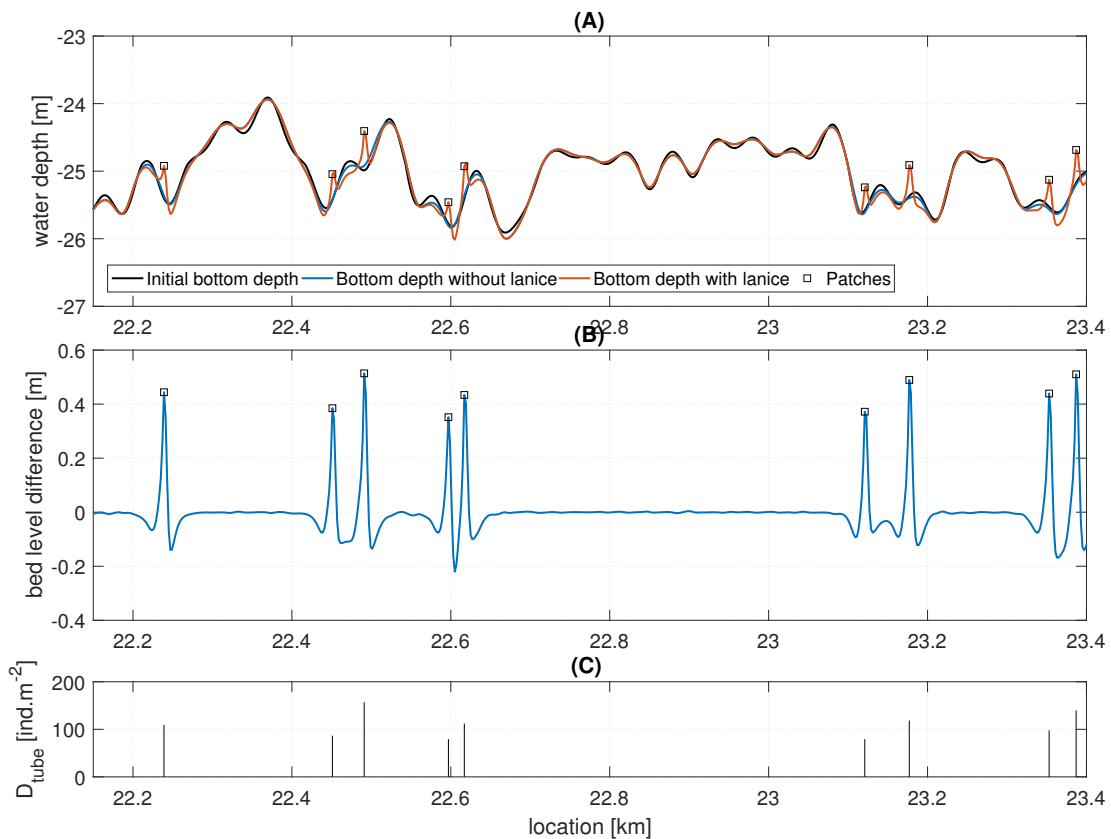


FIGURE 6.12: (A) Morphological development after one year with and without patches. (B) Bed level difference between the bottom with and without patches. (C) Tube densities at every patch in autumn.

Two main differences are found compared with the sinusoidal bottom. First of all, tubes can settle on local crests in this model. The reason therefor is that the bed shear stress at these local crests is still lower than the average bed shear stress in the whole domain. The second difference is about the tube densities observed in the troughs. The tube densities in the troughs of the self-organisational bottom are more variable than in the troughs of the sinusoidal bottom. The troughs of the self-organisational bottom are not all on the same height (at the y-axis), which is the

case for the sinusoidal bottom. This means that sediment factors can be higher in troughs of the self-organisational bottom than in troughs of the sinusoidal bottom. In the self-organisational bottom case the tube densities are more dependent on the specific location, than whether it is a trough or not.

Furthermore, at all places where no patches are present, the bed level is equal to the bed level without patches. This indicates that after one year, the bed levels are only locally changed. This was also shown for the sinusoidal bottom.

Also for this bathymetry, the model is run after the tubes has disappeared, in order to show the degradation rates of the mounds (fig. 6.13). In the first season, a large part of the mound is already disappeared. Subsequently, it is dependent on the location how long it takes to completely disappear. As well as for the sinusoidal bottom, it holds that at locations where the bed shear stress is relatively low, the mounds are more persistent. At local crests and troughs, mounds are more persistent than at flanks.

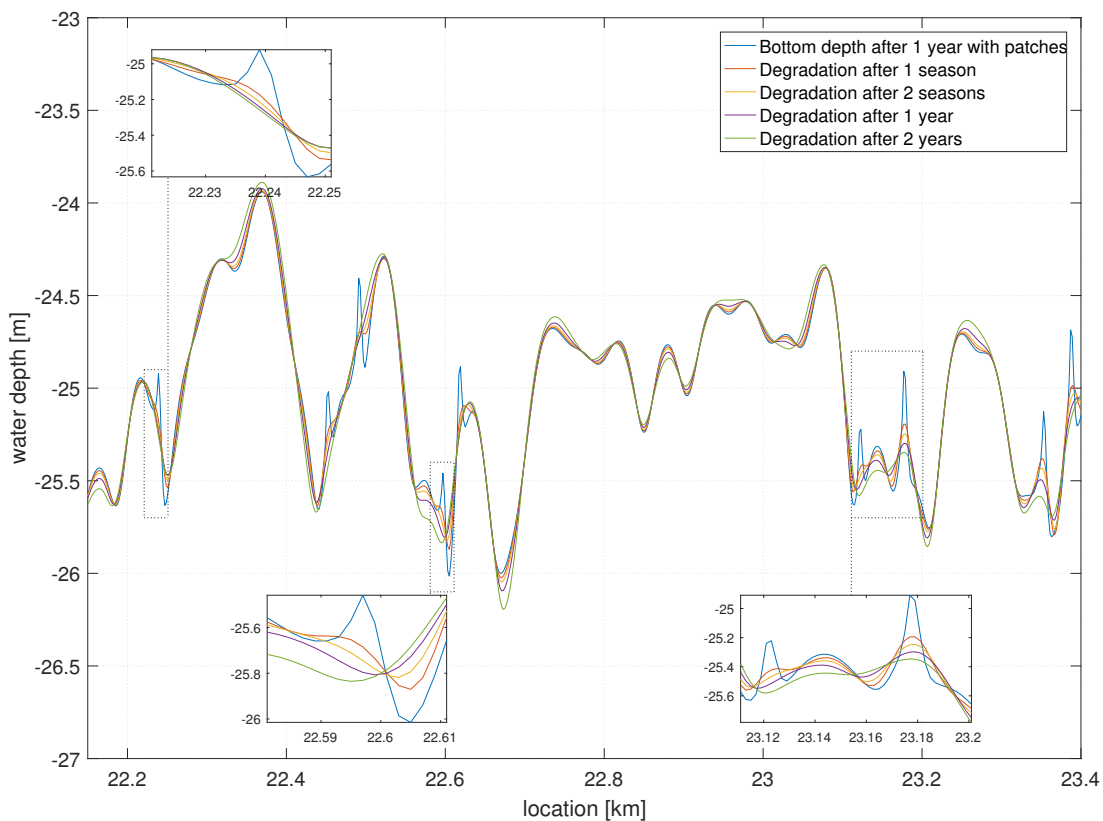


FIGURE 6.13: The degradation of the mounds after all tubes have left the mound.

Option two after twenty years

The morphological development after 20 years is analyzed separately for the two model runs for option two and three (tab. 6.4). For option two, the patches did disappear every year (fig. 6.14). Approximately 28% of the bottom has been covered with patches during 20 years of morphological development. Most of the troughs and crests of the bottom with patches are smaller than the troughs and crest of the bottom without patches. A possible reason therefore is that the tubes prevented the formation of recirculation cells.

The tube densities does not reach the maximum, because the patches disappear every year. The tube densities are dependent on the location.

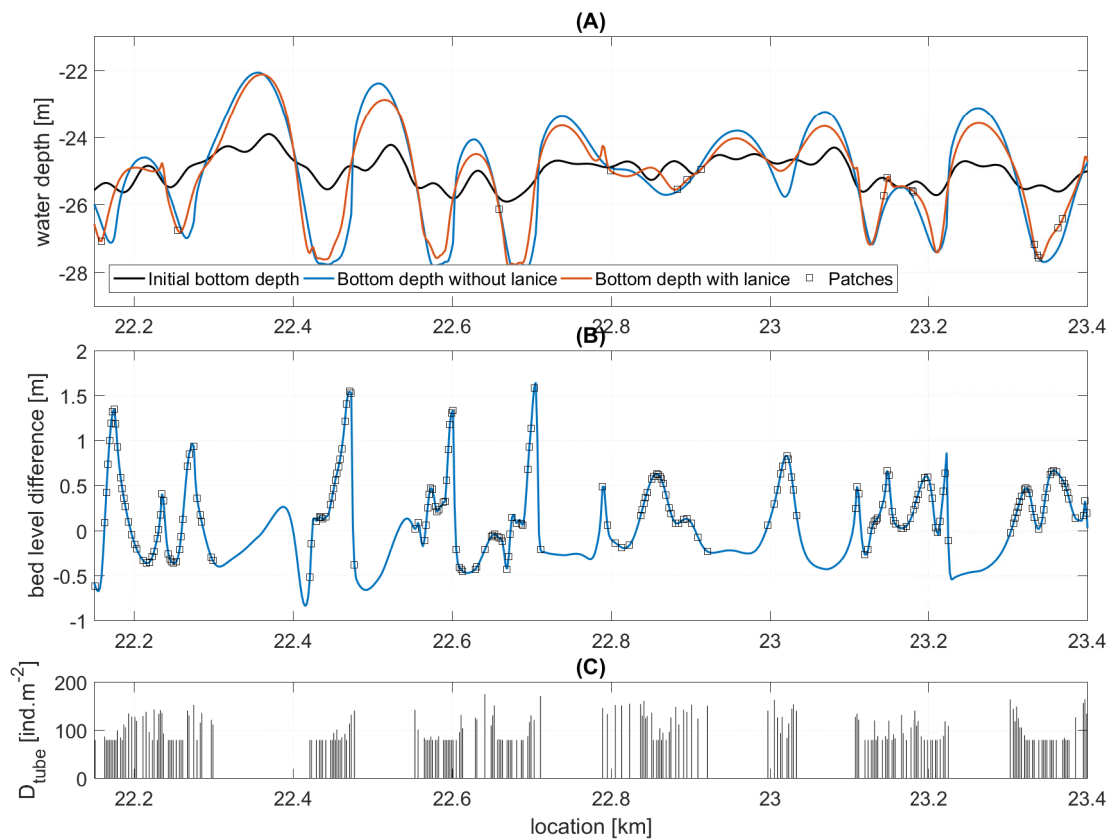


FIGURE 6.14: (A) Morphological development after 20 years where all patches disappear every year (option two). Only the locations of the patches of the last year are shown. (B) Bed level difference with all patches during the 20 years are shown. (C) Densities of all patches during the 20 years.

Option three after twenty years

For the third option (tab. 6.4), every five year all patches disappear (fig. 6.15). Approximately 23% of the bottom has been covered with patches. As well as for the previous model, most of the troughs and crest are smaller than the bottom without patches. However, in this case the patches last longer at one location.

The maximum density observed in this model was 300 ind.m^{-2} , which also is the maximum density. Because the patches last longer at one location, it is possible to grow to the maximum density.

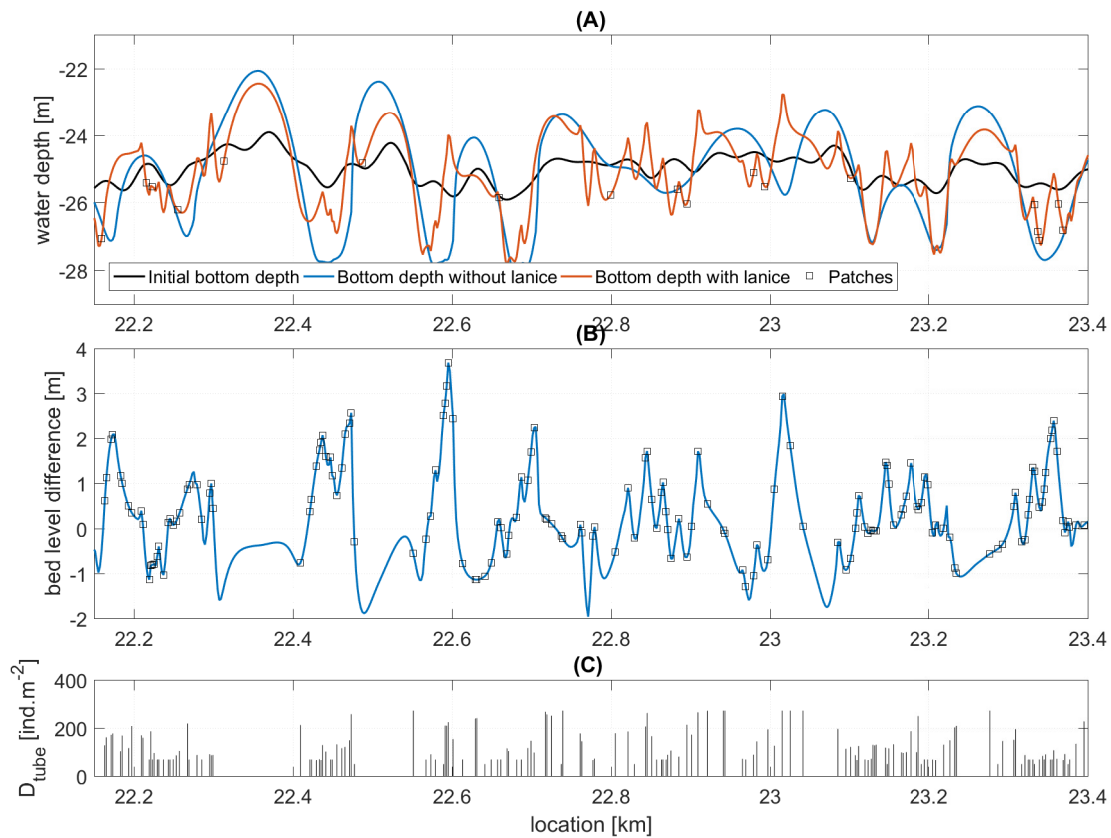


FIGURE 6.15: (A) Morphological development after 20 years where all patches disappear every five years (option three). Only the locations of the patches of the last year are shown. (B) Bed level difference with all patches during the 20 years are shown. (C) Densities of the patches during the 20 years.

Frequency domain

The frequency domain of the self-organisational bottom with and without patches is shown in figure 6.16. For all cases a peak is shown at a wavenumber of 0.003 (wavelength 309 m). The fastest growing mode in this domain is a wavelength of 309 m. Sand waves with a wave length of 309 meter will therefore appear in this model. The range of wave lengths shown, is for all three cases (two cases with and one without patches) approximately equal. The new wavelengths are shown due to the mounds which arise in the domain.

The fastest growing mode of the system, a wave length of 309 meter, is found in all cases. Furthermore, in the case where all patches disappear every five year, a lot of smaller wave lengths are seen compared to the other cases. This is because the mounds are seen as wave lengths.

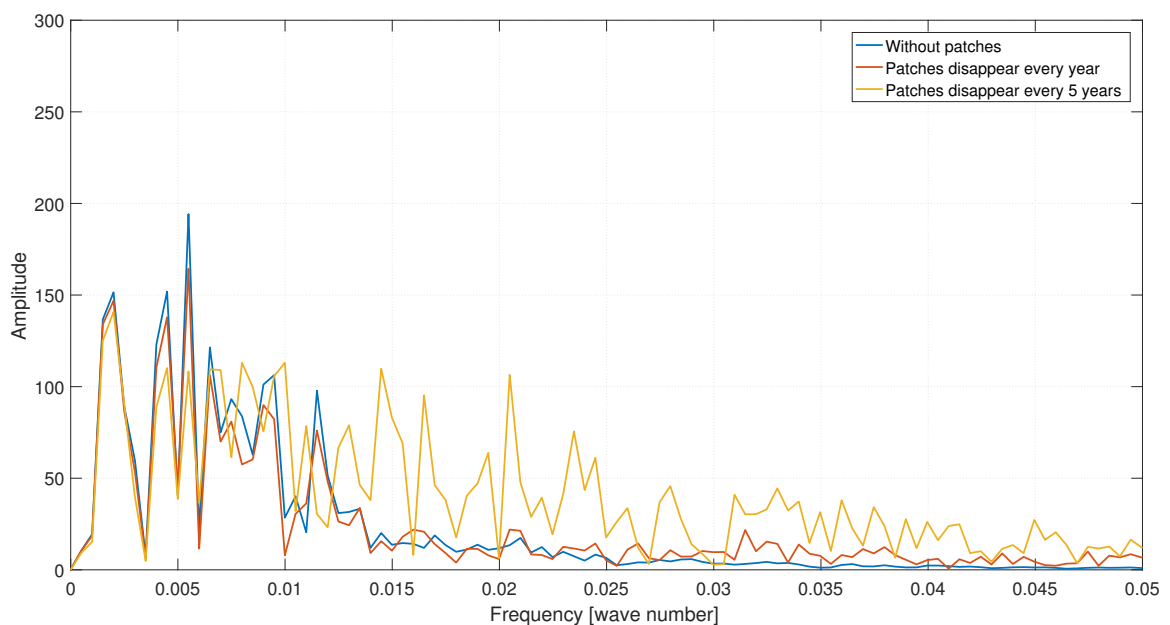


FIGURE 6.16: Periodogram of the morphological development after 10 years.

6.5 Conclusion

After consideration of the two sediment factors, the second was found to be the most realistic one (tab. 6.3). With this factor the tube density within a patch was increasing instead of decreasing, what happened for the first sediment factor. Therefore, this factor has been used for morphological development on the long term. The reason that for the chosen sediment factor the tube densities did increase, was because two restrictions were added to the equations. This ensures that the sediment factor does not become too low.

For one year of morphological development, for both bathymetries, the bed level was only locally changed at the locations of the patches. The mound heights were in agreement with field studies. The degradation rates of the mounds were dependent on the location of the mound, degradation rates were different at the troughs, half-way the flanks and at local crests (only for the self-organizational bottom). The reason therefor is the difference in bed shear stresses.

For the option two and three, where the patches disappeared every five years and never, more sand wave lengths were observed in the spectrum. The small sand wave lengths (large wave numbers) observed were the mounds which were found in the model. For option one, where the patches disappeared every year, the wave lengths were approximately equal to the bottom without patches.

The self-organizational bottom showed a smaller sand wave growth for the bottom with patches compared to the bottom without patches.

CHAPTER 7

Discussion

The effects of a two-way coupling between dynamic patches of *Lanice conchilega* and dynamically active sand waves are determined using the numerical, process based model Delft3D. There are some points of discussion, which are described below.

Grid and bathymetry

The Delft3D model used is run in 2DV. Therefore, the flow can only flow over and through the patch and not around the patch. However, in reality water can also flow around the patch. Furthermore, the vertical layering is divided into 60 and 100 steps. The modeled tubes of *Lanice conchilega* are always the exact length of a certain amount of cumulative layers. It means that the tube length is not always the exact length as has been modeled. For example, in the sand wave model the distance between the layers is different above a trough and a crest. Therefore, the tube lengths are not equal in different grid cells. Moreover, at one grid cell in different seasons the tube length becomes different, because after a mound arise, the vertical layering has another distribution.

Food for the worms

In the model the density is limited by the sediment availability as food for the worms. This model suggest that in the troughs there is less food available, so the density is limited. However, the case study of Van Dijk et al. (2012) shows that tidal ridge troughs are poorly sorted and muddy. This has been shown for sand waves as well by Roos et al. (2007). This suggests that there is enough food available in the troughs, but in this model it is not, and especially not in the sand waves with larger sand wave heights. In this model, there is chosen to set restrictions to the sediment factor, so that the tube density grows in every season. It is shown that the tube densities in the troughs are lower than half-way the flanks. If the studies of Roos et al. (2007) and Van Dijk et al. (2012) are taken into account, however, the densities should be higher in the troughs and lower half-way the flanks.

Density and lasting of patches

Exactly in every season (winter, spring, summer, autumn) the density of the patch has been updated. However, in real life the patch adapts gradually and not specifically at some time step. Strasser and Pieloth (2001) studied the recolonization pattern of a *Lanice conchilega* patch after a severe winter, in which all tubes died. After three years the population was fully recovered. However, other researchers (Callaway et al., 2010; Rabaut et al., 2009) suggested *Lanice conchilega* patches to be reefs. Therefore not all worms will disappear during winter. The mortality rate of the worms

can be dependent on the water temperature and storm factors. This is not taken into account in this model. The mortality rate in winter used in this model is therefore not exactly based on field studies.

One option was that all patches disappear every year, where in the other option all patches disappear every five years. This was based on the field studies of Strasser and Pieloth (2001), Rabaut et al. (2009), and Callaway et al. (2010). The results showed that the mounds of patches which were lasting for more than one year were not in accordance with field values (10-80 cm). However, in reality, recruitment in patches which were destroyed by low water temperatures, was low in the first two years. After the third year they were fully recovered (Strasser and Pieloth, 2001). These mounds were lasting for more than one year, but they did not reach larger mounds heights than 80 cm. The reason that the patches grow too high in this model, is that the tubes do not stop growing, where they do in reality.

Location of patches

The parameter used in the model to determine where patches would settle was only the bed shear stress. Patches were settled where the tide-averaged bed shear stress was lower than the tide-averaged bed shear stress averaged over the whole domain. To determine where the patches would settle, the available mud and sediment sorting was not taken into account. It was not possible to determine the available mud, because a non-cohesive sediment was used. Furthermore it was not possible to determine the sorting of sediment, because only one grain size has been used. However, Herman et al. (2001) concluded that both situations are present at the same location, therefore using only one indicator gives a good representation of the preferred location of the worms.

Time scale

This model requires a lot of computational time, because the time scale of the biology is much smaller than the time scale of the geomorphology. The model has to be adapted to the biological time scale, because otherwise the dynamic patches of *Lanice conchilega* could not be implemented into the model. Due to the small biological time scale, the model requires much computational time.

Realistic settings

The conditions implemented in the Delft3D model are calm, summer conditions. However, in reality also other conditions are possible. For example waves and storms, which can cause damage to the *Lanice conchilega* reefs. These severe conditions are not taken into account in this model. During storms, current velocities can become larger, and therefore, mounds can be more easily eroded. Furthermore, waves can possibly also erode sediments from a mound, because larger flow velocities exist in waves.

Generalisation

This research has only been done for the tube-building species *Lanice conchilega*. However, the results can also be valid for other species, which have approximately the same characteristics as *Lanice conchilega*. The models are run in the sub tidal area. It was not possible to run it for inter tidal areas, because the drying and flooding gives numerical errors in Delft3D. These results are especially made for the sub tidal area, the results for inter tidal areas will be somewhat different. Species which also forms reefs and mounds are mussels and oysters.

 CHAPTER 8

Conclusion and recommendations

8.1 Conclusion

This section briefly gives an answer on the research questions as stated in section 1.2. The research objective is formulated as follows:

*Determine the effects of a two-way coupling between dynamic patches of *Lanice conchilega* and dynamically active sand waves, by using the process-based model Delft3D.*

The answers are given for each question:

What is the influence of patches of *Lanice conchilega* on the sediment transport rates on a flat bed for varying tube densities, tube lengths and patch sizes?

Patches with tubes of *Lanice conchilega* are able to change the hydrodynamics and therewith the sediment dynamics. The hydrodynamics determine for a large part the sediment dynamics, therefore the variations in tube length, density, patch length, and distance between two patches are only done for the hydrodynamic case. The rate of influence of a patch on the flow velocity and bed shear stress is dependent on the tube length, density, patch length and distance between two patches. The tube density is the most important factor for the bed shear stress to decrease, although the effect decreases for increasing densities. The reason therefore is the hiding-effect.

Mounds are formed on the flat bottom, this is caused by sediment which is trapped between the tubes. Within the patch the bed load transport becomes much lower, through which it settles. The suspended sediment concentration within the patch decreases because it is settled down. The variation of sediment transport is equal to the variation in hydrodynamics.

In this research, only the tube-building worm *Lanice conchilega* has been investigated. However, the effects are also valid for other species which protrude from the sediment.

How can the distribution of patches of *Lanice conchilega* be explained by the physical conditions along the sand wave crest, trough and flank?

Two parameters determining the location of patches of *Lanice conchilega* are bed shear stress and the % mud content (Herman et al., 2001; Willems et al., 2008).

The spreading of marine habitats over tidal sand ridges is presented by Van Dijk et al. (2012). The well-sorted crests have communities which are low in density and diversity. The troughs were poorly sorted and muddy, with communities high in

density and diversity. These well-sorted crests and less well-sorted troughs are also found in sand waves (Roos et al., 2007). Furthermore Herman et al. (2001) concludes that muddy situations and a low bed shear stress are both present at the same location.

This suggests that patches of *Lanice conchilega* will settle at troughs and lower flanks of sand waves, where bed shear stress is low and mud is available.

This determination of the preferred location to settle could also be used for other species, considering that the bed shear stress is an indicator for the presence of various species (Herman et al., 2001; De Jong et al., 2015).

What is the influence of the interaction between dynamic patches of *Lanice conchilega* and sand wave dynamics on the growth of sand waves?

The sinusoidal and self-organizational bottom were run with three options. The patches did never disappear, they did disappear every year and they did disappear every five years. The model where all patches disappeared every year was the most realistic model. The mound heights were comparable to field values. The wave length after ten years of morphological development with patches was approximately equal to the wave length without patches.

After one year of morphological development the bed levels were only locally changed at the locations of the patches. This was shown both for the sinusoidal and self-organizational bottom. After twenty years of morphological development the self-organizational bottom showed a smaller sand wave growth for the bottom with patches compared to the bottom without patches.

8.2 Recommendations

This section gives some recommendations with regard to this research.

Parameterization

Due to the amount of layers and grid cells, this model requires a large computational time. A different layer distribution could have been used, however, the layers close to the bottom are important to describe the processes close to the bottom. Furthermore, the length of *Lanice conchilega* is dependent on the vertical layer width. Because the average surface area of the patches found in the field is 1.37 m² (Rabaut, 2009), it is not possible to decrease the grid cell width. The grid cell used in this model is already a little bit too large, however this decreased the computational time drastic.

In order to speed up the computational time, a parameterization for *Lanice conchilega* can be used. Instead of modeling the tubes, which required a lot of vertical layers, only the influence on the hydrodynamics can be implemented (Borsje et al., 2009c).

The two time scales used in this research are very different. The biology changes on a small time scale in months, whereas the morphodynamics changes on large time scales in years. It is important to find ways how this can be implemented into the modeling.

Migration of sand waves

In this model only the effects of living patches with *Lanice conchilega* on the growth of sand waves has been studied. However in the field, sand waves also migrate. A

question what arises here is, do the patches move, or do they end up in the crest of the sand wave. Initially, patches will not settle at crests, because the bed shear stress is too large. So there should be investigated what happens when the sand waves migrate. Future research should also focus on the migration of sand waves and how the patches behave in a migrating sand wave.

Suspended sediment as food

In this model the suspended sediment is used as the available food for the worms. Two restrictions are used, such that the density increases. However, in the troughs the density becomes smaller than half-way the flanks. Future research should focus on a way to implement the sediment as food according to the sorting of sediment into sand waves. Where troughs are less-sorted and crests are well-sorted.

Bibliography

- Bagnold, R.A. (1956). "The flow of cohesionless grains in fluids". In: *Philosophical Transactions of the Royal Society A: Mathematical, Physical and Engineering Sciences* 249.964, pp. 235–297.
- Bärenbold, F., B. Crouzy, and P. Perona (2016). "Stability analysis of ecomorphodynamic equations". In: *Water Resources Research* 52, pp. 7548–7555. ISSN: 00431397. arXiv: 2014WR016527 [10.1002].
- Besio, G., P. Blondeaux, and P. Frisina (2003). "A note on tidally generated sand waves". In: *Journal of Fluid Mechanics* 485.2003, pp. 171–190. ISSN: 00221120.
- Besio, G., P. Blondeaux, M. Brocchini, and G. Vittori (2004). "On the modeling of sand wave migration". In: *Journal of Geophysical Research C: Oceans* 109, p. C04018. ISSN: 01480227.
- Besio, G., P. Blondeaux, and G. Vittori (2006). "On the formation of sand waves and sand banks". In: *Journal of Fluid Mechanics* 557, pp. 1–27. ISSN: 1469-7645.
- Besio, G., P. Blondeaux, M. Brocchini, S.J.M.H. Hulscher, D. Idier, M.A.F. Knaapen, A.A. Németh, P.C. Roos, and G. Vittori (2008). "The morphodynamics of tidal sand waves: A model overview". In: *Coastal Engineering* 55, pp. 657–670. ISSN: 03783839.
- Beukema, J.J., W. De Bruin, and J.J.M. Jansen (1978). "Biomass and species richness of the macrobenthic animals living on the tidal flats of the Dutch Wadden Sea: Long-term changes during a period with mild winters". In: *Netherlands Journal of Sea Research* 12.1, pp. 58–77.
- Bhaud, M. (2000). "Two contradictory elements determine invertebrate recruitment: dispersion of larvae and spatial restrictions on adults". In: *Oceanologica Acta* 23.4, pp. 409–422.
- Bhaud, M.R. and C.P. Cazaux (1990). "Buoyancy characteristics of *Lanice conchilega* (Pallas) larvae (Terebellidae). Implications for settlement". In: *Journal of Experimental Marine Biology and Ecology* 141.1, pp. 31–45.
- Blondeaux, P. and G. Vittori (2005a). "Flow and sediment transport induced by tide propagation: 1. The flat bottom case". In: *Journal of Geophysical Research C: Oceans* 110, p. C07020. ISSN: 01480227.
- (2005b). "Flow and sediment transport induced by tide propagation: 2. The wavy bottom case". In: *Journal of Geophysical Research C: Oceans* 110, p. C08003. ISSN: 01480227.
- Borsje, B.W. (2012). "Biogeomorphology of coastal seas; How benthic organisms, hydrodynamics and sediment dynamics shape tidal sand waves". PhD thesis. University of Twente. (UTwente). ISBN: 9789036534345.
- Borsje, B.W., G. Besio, P. Blondeaux, P. Hulscher, and G. Vittori (2008). "Exploring biological influence on offshore sandwave length". In: *Marine and River Dune Dynamic III, International Workshop*, pp. 31–38.

- Borsje, B.W., M.B. De Vries, T.J. Bouma, G. Besio, S.J.M.H. Hulscher, and P.M.J. Herman (2009a). "Modeling bio-geomorphological influences for offshore sandwaves". In: *Continental Shelf Research* 29.9, pp. 1289–1301. ISSN: 02784343.
- Borsje, B.W., M.C. Buijsman, G. Besio, M.B. De Vries, S.J.M.H. Hulscher, P.M.J. Herman, and H. Ridderinkhof (2009b). "On the modeling of bio-physical influences on seasonal variation in sandwave dynamics". In: *Journal of Coastal Research* 2009.56.
- Borsje, B.W., S.J.M.H. Hulscher, P.M.J. Herman, and M.B. De Vries (2009c). "On the parameterization of biological influences on offshore sand wave dynamics". In: *Ocean Dynamics* 59.5, pp. 659–670. ISSN: 16167341.
- Borsje, B.W., P.C. Roos, W.M. Kranenburg, and S.J.M.H. Hulscher (2013). "Modeling tidal sand wave formation in a numerical shallow water model: The role of turbulence formulation". In: *Continental Shelf Research* 60, pp. 17–27. ISSN: 02784343.
- Borsje, B.W., T.J. Bouma, M. Rabaut, P.M.J. Herman, and S.J.M.H. Hulscher (2014a). "Formation and erosion of biogeomorphological structures: A model study on the tube-building polychaete *Lanice conchilega*". In: *Limnology and Oceanography* 59.4, pp. 1297–1309. ISSN: 00243590.
- Borsje, B.W., W.M. Kranenburg, P.C. Roos, J. Matthieu, and S.J.M.H. Hulscher (2014b). "The role of suspended load transport in the occurrence of tidal sand waves". In: *Journal of Geophysical Research: Earth Surface* 119. ISSN: 21699011.
- Buhr, K.J. (1976). "Suspension-Feeding and Assimilation Efficiency in *Lanice conchilega* (Polychaeta)*". In: *Marine Biology* 38, pp. 373–383.
- Burchard, H., P.D. Craig, J.R. Gemmrich, H. van Haren, P.-P. Mathieu, H.E.M. Meier, W.A.M.N. Smith, H. Prandke, T.P. Rippeth, E.D. Skillingstad, William D. Smyth, David J.S. Welsh, and H.W. Wijesekera (2008). "Observational and numerical modeling methods for quantifying coastal ocean turbulence and mixing". In: *Progress in Oceanography* 76.4, pp. 399–442.
- Callaway, R. (2003). "Juveniles stick to adults: recruitment of the tube-dwelling polychaete *Lanice conchilega* (Pallas, 1766)". In: *Hydrobiologia* 503, pp. 121–130.
- Callaway, Ruth, Nicolas Desroy, Stanislas F. Dubois, J??r??me Fournier, Matthew Frost, Laurent Godet, Vicki J. Hendrick, and Marijn Rabaut (2010). "Ephemeral bio-engineers or reef-building polychaetes: How stable are aggregations of the tube worm *lanice conchilega* (Pallas, 1766)?" In: *Integrative and Comparative Biology* 50.2, pp. 237–250. ISSN: 15407063.
- Carey, D.A. (1987). "Sedimentological effects and palaeoecological implications of the tube-building polychaete *Lanice conchilega* Pallas". In: *Sedimentology* 34.1, pp. 49–66.
- Corenblit, D., A.C.W. Baas, G. Bornette, J. Darrozes, S. Delmotte, R.A. Francis, A.M. Gurnell, F. Julien, R.J. Naiman, and J. Steiger (2011). "Feedbacks between geomorphology and biota controlling Earth surface processes and landforms: A review of foundation concepts and current understandings". In: *Earth-Science Reviews* 106.3-4, pp. 307–331. ISSN: 00128252.
- Crouzy, B., F. Bärenbold, P. D'Odorico, and P. Perona (2016). "Ecomorphodynamic approaches to river anabranching patterns". In: *Advances in Water Resources* 93, pp. 156–165. ISSN: 03091708.
- Damveld, J.H., B.W. Borsje, P.C. Roos, and S.J.M.H. Hulscher (2015). "Smart and sustainable design for offshore operations in a sandy seabed - the SANDBOX programme". In: *Marid V* April.
- De Jong, M.F., M.J. Baptist, H.J. Lindeboom, and P. Hoekstra (2015). "Relationships between macrozoobenthos and habitat characteristics in an intensively used area of the Dutch coastal zone". In: *ICES Journal of Marine Science* 72.8, pp. 2409–2422. ISSN: 10959289.

- Degraer, S., E. Verfaillie, W. Willems, E. Adriaens, M. Vincx, and V. Van Lancker (2008). "Habitat suitability modelling as a mapping tool for macrobenthic communities: An example from the Belgian part of the North Sea". In: *Continental Shelf Research* 28.3, pp. 369–379.
- Forster, S. and G. Graf (1995). "Impact of irrigation on oxygen flux into the sediment: intermittent pumping by *Callianassa subterranea* and ?piston-pumping? by *Lanice conchilega*". In: *Marine Biology* 123.2, pp. 335–346.
- Friedrichs, M., G. Graf, and B. Springer (2000). "Skimming flow induces over a simulated polychaete tube lawn at low population densities". In: *Mar. Ecol. Prog. Ser.* 192, pp. 219–228.
- Gerkema, T. (2000). "A linear stability analysis of tidally generated sand waves". In: *J. Fluid Mech* 417, pp. 303–322.
- Heimler, W. (1981). "Untersuchungen zur larvalentwicklung von *Lanice conchilega* (Pallas, 1766) (Polychaeta, Terebellomorpha), Teil I: Entwicklungsablauf". In: *Zool. JB. Anat.* 106, pp. 12–45.
- Herman, P.M.J., J.J. Middelburg, and C.H.R. Heip (2001). "Benthic community structure and sediment processes on an intertidal flat: results from the ECOFLAT project". In: *Continental Shelf Research* 21.18-19, pp. 2055–2071.
- Heuers, J. and S. Jaklin (1999). "Initial Settlement of *Lanice conchilega*". In: *Senckenbergiana marit* 29, pp. 67–69.
- Heuers, J., S. Jaklin, R. Zuhlke, S. Dittmann, C.P. Gunther, H. Hildenbrandt, and V. Grimm (1998). "A model on the distribution and abundance of the tube building polychaete *Lanice conchilega* (Pallas, 1766) in the intertidal of the Wadden Sea." In: *Verhandl Ges fur Ökol* 28, pp. 207–215.
- Holthe, T. (1978). "The zoogeography of the Terebellomorpha (Polychaeta) of the northern European waters". In: *Sarsia* 63.3, pp. 191–198.
- Hulscher, S.J.M.H. (1996). "Tidal-induced large-scale regular bed form patterns in a three-dimensional shallow water model". In: *Journal of Geophysical Research* 101, pp. 20,727–20,744.
- Huthnance, J.M. (1982). "On one mechanism forming linear sand banks". In: *Estuarine, Coastal and Shelf Science* 14.1, pp. 79–99. ISSN: 02727714.
- Jones, C.G., J.H. Lawton, and M. Shachak (1994). "Organisms as Ecosystem Engineers". In: *OIKOS* 69.3, pp. 373–386.
- Jones, S. E. and C. F. Jago (1993). "In situ assessment of modification of sediment properties by burrowing invertebrates". In: *Marine Biology* 115.1, pp. 133–142.
- Kessler, M. (1963). "Die Entwicklung von *Lanice conchilega* (Pallas) mit besonderer Berücksichtigung der Lebensweise". In: *Helgol. Wiss. Meeresunters* 8, pp. 425–476.
- Komarova, N.L. and S.J.M.H. Hulscher (2000). "Linear instability mechanisms for sand wave formation". In: *J. Fluid Mech* 413, pp. 219–246.
- Lesser, G.R., J.A. Roelvink, J.A.T.M. Van Kester, and G.S. Stelling (2004). "Development and validation of a three-dimensional morphological model". In: *Coastal Engineering* 51.8-9, pp. 883–915.
- Meadows, P.S., A. Meadows, and J.M.H. Murray (2012). "Biological modifiers of marine benthic seascapes: Their role as ecosystem engineers". In: *Geomorphology* 157, pp. 31–48.
- Murray, A.B., M.A.F. Knaapen, M. Tal, and M.L. Kirwan (2008). "Biomorphodynamics: Physical-biological feedbacks that shape landscapes". In: *Water Resources Research* 44.11, W11301.
- Németh, A.A., S.J.M.H. Hulscher, and H.J. de Vriend (2002). "Modelling sand wave migration in shallow shelf seas". In: *Continental Shelf Research* 22, pp. 2795–2806. ISSN: 02784343.

- Németh, A.A., S.J.M.H. Hulscher, and R.M.J. Van Damme (2007). "Modelling offshore sand wave evolution". In: *Continental Shelf Research* 27, pp. 713–728. ISSN: 02784343.
- Nicolaidou, A. (2003). "Observations on the re-establishment and tube construction by adults of the polychaete *Lanice conchilega*". In: *Journal of the Marine Biological Association of the United Kingdom*, pp. 1223–1224.
- Petersen, B. and K.-M. Exo (1999). *Predation of waders and gulls on *Lanice conchilega* tidal flats in the Wadden Sea*.
- Rabaut, M. (2009). "Lanice conchilega, fisheries and marine conservation: Towards an ecosystem approach to marine management". PhD thesis. Ghent University (UGent), p. 354. ISBN: 9789087560256.
- Rabaut, M., K. Guilini, G. Van Hoey, M. Vincx, and S. Degraer (2007). "A bio-engineered soft-bottom environment: The impact of *Lanice conchilega* on the benthic species-specific densities and community structure". In: *Estuarine, Coastal and Shelf Science* 75.4, pp. 525–536. ISSN: 02727714.
- Rabaut, M., M. Vincx, and S. Degraer (2009). "Do *Lanice conchilega* (sandmason) aggregations classify as reefs? Quantifying habitat modifying effects". In: *Helgoland Marine Research* 63.1, pp. 37–46. ISSN: 1438387X.
- Rodi, W. (1984). *Turbulence models and their application in hydrodynamics: A state of the art review*. Univ. of Karlsruhe, Karlsruhe, Germany.
- Roos, P.C., S.J.M.H. Hulscher, F. Van Der Meer, T.A.G.P. Van Dijk, I.G.M. Wientjes, and J. Van Den Berg (2007). "Grain size sorting over offshore sandwaves: observations and modelling". In:
- Ropert, M. and J.C. Dauvin (2000). "Renewal and accumulation of a *Lanice conchilega* (Pallas) population in the baie des Veys, western Bay of Seine". In: *Oceanologica Acta* 23.4, pp. 529–546.
- Sekine, M. and G. Parker (1992). "Bed-load transport on transverse slope". In: *Journal of Hydraulic Engineering* 118.4, pp. 513–535.
- Sterlini, F., S.J.M.H. Hulscher, and D.M. Hanes (2009). "Simulating and understanding sand wave variation: A case study of the Golden Gate sand waves". In: *J. Geophys. Res* 114, p. 15.
- Strasser, M. and U. Pieloth (2001). "Recolonization pattern of the polychaete *Lanice conchilega* on an intertidal sand flat following the severe winter of 1995/96". In: *Helgol Mar Res* 55, pp. 176–181.
- Temmerman, S., T.J. Bouma, G. Govers, Z.B. Wang, M.B. De Vries, and P.M.J. Herman (2005). "Impact of vegetation on flow routing and sedimentation patterns: Three dimensional modeling for a tidal marsh". In: *Journal of Geophysical Research* 110.4, pp. 1–18.
- Uittenbogaard, R. (2003). "Modelling turbulence in vegetated aquatic flows". In: *International workshop on RIParian FORest vegetated channels: hydraulic, morphological and ecological aspects*.
- Van Oyen, T. and P. Blondeaux (2008). "Grain sorting effects on the formation of sand waves". In: *Marine and River Dune Dynamics*, pp. 249–256.
- Van Dijk, T.A.G.P., J.A. van Dalen, V. van Lancker, R.A. van Overmeeren, S. van Heteren, and P.J. Doornenbal (2012). "Benthic habitat variations over tidal ridges, North Sea, the Netherlands". In: *Seafloor Geomorphology as Benthic Habitat*, pp. 241–249.
- Van Gerwen, W., B.W. Borsje, J.H. Damveld, and S.J.M.H. Hulscher (2016). "Modelling the effect of suspended load transport and tidal asymmetry on the growth of tidal sand wave fields". In:

- Van Hoey, G. (2006). "Spatio-temporal variability within the macrobenthic *Alba alba* community, with emphasis on the structuring role of *Lanice conchilega*". PhD thesis. Ghent University (UGent), p. 187.
- Van Hoey, G., M. Vincx, and S. Degraer (2006). "Some recommendations for an accurate estimation of *Lanice conchilega* density based on tube counts". In: *Helgoland Marine Research* 60, pp. 317–321.
- Van Hoey, G., K. Guilini, M. Rabaut, M. Vincx, and S. Degraer (2008). "Ecological implications of the presence of the tube-building polychaete *Lanice conchilega* on soft-bottom benthic ecosystems". In: *Marine Biology* 154.6, pp. 1009–1019. ISSN: 00253162.
- Van Rijn, L.C. (2007). "Unified View of Sediment Transport by Currents and Waves. II: Suspended Transport". In: *Journal of Hydraulic Engineering* 133.6, pp. 668–689.
- Van Rijn, L.C., D.J.R. Walstra, and M. van Ormondt (2004). *Description of TRANSPOR2004 and implementation in Delft3D-ONLINE : final report - Publicatiedatabank IenM*. Tech. rep. Delft, Netherlands: Delft Hydraul, Z3748.
- Widdows, J. and M. Brinsley (2002). "Impact of biotic and abiotic processes on sediment dynamics and the consequences to the structure and functioning of the intertidal zone". In: *Journal of Sea Research* 48.2, pp. 143–156. ISSN: 13851101.
- Willems, W., P. Goethals, D. Van den Eynde, G. Van Hoey, V. Van Lancker, E. Verfaille, M. Vincx, and S. Degraer (2008). "Where is the worm? Predictive modelling of the habitat preferences of the tube-building polychaete *Lanice conchilega*". In: *Ecological Modelling* 212.1-2, pp. 74–79. ISSN: 03043800.
- Ziegelmeier, E. (1952). "Beobachtungen über den Rohrenbau von *Lanice conchilega* {PALLAS} im Experiment und am natürlichen Standort". In: *Helgolander wiss Meeresunters* 46, pp. 261–272.
- Zühlke, R. (2001). "Polychaete tubes create ephemeral community patterns: *Lanice conchilega* (Pallas, 1766) associations studied over six years". In: *Journal of Sea Research* 46.3-4, pp. 261–272. ISSN: 1385-1101.